MOLECULAR AND CELLULAR BIOLOGY, Oct. 2008, p. 6358–6372 Vol. 28, No. 20
0270-7306/08/$08.00+0 doi:10.1128/MCB.00333-08


# Effects of the SANT Domain of Tension-Induced/Inhibited Proteins (TIPs), Novel Partners of the Histone Acetyltransferase p300, on p300 Activity and TIP-6-Induced Adipogenesis▽

Kameswara Rao Badri, Yuanxiang Zhou, Urmil Dhru, Sreelatha Aramgam, and Lucia Schuger*

*Department of Pathology, Wayne State University, School of Medicine, Detroit, Michigan 48201*

Received 27 February 2008/Returned for modification 8 May 2008/Accepted 4 August 2008

**We previously identified a set of transcription regulators, referred to as TIPs (*t*ension-*i*nduced/inhibited *p*roteins), with a role in myogenic versus adipogenic differentiation. Here we report that the TIP family comprises eight isoforms, all bearing a SANT (*s*witching-defective protein 3, *a*daptor 2, *n*uclear receptor corepressor, and *t*ranscription factor IIIB) domain and some of them presenting *S*-adenosyl-L-methionine (SAM) and nuclear receptor box (NRB) motifs, all characteristic of histone-modifying enzymatic complexes. TIPs have SANT-dependent, p300-mediated histone acetyltransferase (HAT) activity. Ectopic TIP-6 ($SANT^+$ $SAM^-$ $NRB^-$) but not TIP-6ΔSANT induced de novo PPARγ2-mediated adipogenic gene expression in NIH 3T3 cells and promoted preadipocyte differentiation into fat cells. TIP-6 was also involved in mediating hormonally/biochemically induced adipogenic differentiation of 3T3-L1 cells. Furthermore, TIP-6 was identified in adipose tissue in vivo. TIP-6 bound directly and indirectly to p300 and histone H4 (H4). Deletion of the SANT domain did not abolish TIP-6 interaction with p300 and H4 but eliminated direct TIP-6 binding to p300. Chromatin immunoprecipitation assays showed the recruitment of TIP-6, TIP-6ΔSANT, and p300 to the PPARγ2 promoter, but H3/H4 acetylation occurred only when p300 was directly associated with TIP-6. These studies demonstrated the importance of TIPs in the recruitment of p300 to specific promoters and in the regulation of p300 HAT activity through the involvement of the SANT domain. Furthermore, we identified TIP-6 as a new member of the adipogenic cascade.**

We originally identified TIP-1 (*t*ension-*i*nduced/inhibited *p*rotein *1*) and TIP-3 in mouse lung embryonic mesenchymal cells while studying the effects of mechanical tension in mesenchymal cell lineage determination (26). TIP-1 was induced upon stretching, a critical signal for smooth muscle differentiation (59); it associated with the promoter of serum response factor (SRF), a key myogenic transcription factor (7), and induced myogenesis. On the contrary, TIP-3 was suppressed by stretching. In nonstretched lung embryonic mesenchymal cells, TIP-3 was recruited to the promoter of peroxisome proliferator-activated receptor gamma 2 (PPARγ2), a key adipogenic transcription factor (43), and induced adipogenesis. Smooth muscle cells and lipofibroblasts are normally present in the lung (36). TIP-2 was found in a GenBank search, but since it was not present in embryonic mesenchymal cells, its function was not studied (26).

Here we report that the TIP family is presently composed of eight isoforms generated by alternative splicing from a single gene located in chromosome 2q22-23 in mice and 2q31.1 in humans. TIPs have nuclear localization signals (NLS), translocate between the nucleus and the cytoplasm (26), and have several previously characterized functional domains. These include a SANT (*s*witching-defective protein 3 [Swi3], *a*daptor 2 [Ada2], *n*uclear receptor corepressor [N-CoR], and *t*ranscription factor IIIB [TFIIIB]) domain, a SAM motif (the D/ExGxGxGx signature motif found in *S*-*a*denosyl-L-*m*ethionine-binding proteins), and an NRB site (*n*uclear *r*eceptor *b*ox, represented by the LXXLL signature motif). These functional domains are characteristically present in catalytic and noncatalytic subunits of histone-modifying enzymatic complexes.

Histone-modifying enzymatic complexes catalyze the covalent attachment or removal of posttranslational modifications, which occur mainly at the N-terminal tails of core histones. These modifications function to decondense chromatin and/or recruit other enzymes or proteins to the nucleosomes, thereby playing an essential role in transcription regulation (8, 31, 34). The most extensively studied modifications are acetylation, deacetylation, and methylation. Histone acetylation has been almost invariably associated with gene activation, while histone deacetylation has been associated with gene silencing (8, 31, 34). Histone methylation has been associated either with activation or silencing depending on the methylated amino acid, its localization in the core histones, and its degree of methylation (8, 31, 34).

The SANT domain is present in all TIP isoforms. This domain was originally identified based on its homology to the DNA binding domain of c-Myb and is comprised of an approximately 50-amino-acid motif characterized by the presence of conserved hydrophobic and aromatic residues in each of three α helices arranged in tandem (1). Despite its similarity to the DNA binding site of c-Myb, the SANT domain lacks several key residues that contact DNA in the Myb DNA-binding domain and contain consecutive hydrophobic residues in the recognition helix that are incongruent with DNA binding (11).

Since its original description, the SANT domain has been identified in multiple histone-modifying enzymatic complexes

* Corresponding author. Mailing address: Department of Pathology, Wayne State University, School of Medicine, 540 E. Canfield Street, Detroit, MI 48201. Phone: (313) 577-5651. Fax: (313) 577-0057. E-mail: lschuger@med.wayne.edu.

▽ Published ahead of print on 18 August 2008.

with histone acetyltransferase (HAT) activity, such as ADA, SAGA, and ATAC in yeast and STAGA, PCAF, and TFTC in mammals (4, 6, 10, 21, 50); histone deacetylase (HDAC) activity, such as silencing mediator of retinoic acid and thyroid hormone receptor (SMRT), complex cI/CoREST, and complex cII (16, 22, 25, 61, 62); and histone methyltransferase (HMT) activity, such as the EED/EZH2 complex (GenBank search). Within these complexes, the SANT domain has been found in catalytic subunits, as in the case of EZH2, as well as in noncatalytic subunits, as in the case of Ada2.

Several studies demonstrated the essential role of the SANT domain in the functioning of histone-modifying enzymatic complexes (6, 10, 22, 50). For example, a SANT domain in Ada2p binds to histone tails and thereby enhances the catalytic efficiency of the Gcn5p-Ada2p complex (10). The SANT domain can also function by binding to the catalytic subunit of the histone enzymatic complex (22, 50, 61, 65), such as in the case of SMRT and N-CoR, in which a SANT domain binds to the latent HDAC3 that results in its activation (22, 65). An enzymatic complex subunit can have two SANT domains, with one binding to histone and the other to the catalytic subunit, such as SMRT (62). Alternatively, a single SANT domain can function by binding to both enzyme and substrate, such as the SANT domain in the Ada2 subunit of the SAGA complex, in which a SANT subdomain interacts with histone and the other subdomain interacts with the HAT enzyme Gcn5 (50).

All TIPs except TIP-1 and TIP-6 have SAM domains. This highly conserved signature motif is found in SAM-binding proteins, including HMTs (5, 14, 39, 57), and is involved in their function. A mutation in the SAM site of PRMT1 and PRMT4/CARM1 coactivator-associated arginine HMTs abrogates their HMT and coactivator activities (14, 57). Further supporting a potential HMT role, the SAM motif in TIP-2, TIP-3, TIP-4, and TIP-5 is embedded in a 104-amino-acid-long region with high homology to established methyltransferases (referred to in GenBank as the "methyltransferase domain"), and TIP-1 and TIP-6, although lacking SAM motifs and methyltransferase domains, are highly homologous (30 to 40% identity) to methyltransferases 12 and 2 (GenBank).

TIP-1, TIP-3, TIP-4, and TIP-5 harbor an NRB, the signature motif of nuclear receptor coregulators (24, 32, 56). Nuclear receptors are a family of transcription factors that control gene expression in a ligand-dependent fashion (20, 37). The NRB binds the coregulator to the nuclear receptor through its leucine residues, which dock into the nuclear receptor AP2 hydrophobic cleft (17, 46) and modulates its activity (19, 24, 29, 32, 56). Coregulators are essential components of multiple histone-modifying enzymatic complexes required for nuclear receptor-mediated transcription (reviewed in references 3, 20, and 37). Nuclear receptor coregulators include HATs, such as Gcn5, p300, and PCAF; subunits of HDAC enzymatic complexes, such as N-CoR and SMRT; subunits in ATP-dependent chromatin remodeling complexes, such as Swi/Snf/BRG1; and HMTs, such as CARM1 and PRMT1 (3).

Here we show that TIPs have recruited HAT activity, identify p300 as the recruited HAT enzyme, and demonstrate the role of the SANT domain in the regulation of p300 catalytic activity. Furthermore, we reveal the involvement of TIP-6, the only TIP with a $SANT^+$ $SAM^-$ $NRB^-$ makeup, in the induction of PPARγ2-mediated adipogenesis.

## MATERIALS AND METHODS

**Plasmids.** The cloning of TIP-1, TIP-2, and TIP-3 was previously described (26). TIP-5 to TIP-8 were cloned from C3H/10T1/2 cells (American Type Culture Collection, Manassas, VA) into pCR2.1-TOPO vector (TOPO TA cloning kit; Invitrogen Corp., Carlsbad, CA). C3H/10T1/2 cells were selected because of their multipotential capability to differentiate into a variety of mesenchymal cell lineages (64). TIP-5 was cloned using the primers sense, 5′-CTGCCATCAAG CCTCAGC-3′, and antisense, 5′-ACTTGGTTCAGGGTCCAACC-3′, complementary to the 5′ and 3′ untranslated region of GenBank sequence accession number BC057960. While cloning TIP-5, we identified TIP-4 as an extra band with an additional approximately 150 bp. TIP-6 was cloned using the primer set sense, 5′-ATGAATGTGATTTGGAGAAGTTGC-3′, and antisense, 5′-CACA CTCTCATACAGTACCTCTAGTATTCG-3′, complementary to GenBank sequence accession number AK042669. TIP-7 was cloned using the primers sense, 5′-GTGTCGCTTCACCTGTGTGT-3′, and antisense, 5′-ACTGTGCCTGGG GTTGC-3′, complementary to GenBank sequence accession number AK039461. During the cloning of TIP-7, we identified TIP-8 as an extra band with an additional approximately 450 bp. TIPΔSANT constructs were produced by a QuikChange II site-directed mutagenesis kit (Stratagene, La Jolla, CA) by following the manufacturer's instructions. All the sequences were verified by sequencing.

**Lentivirus constructs.** Sequences expressing scrambled short hairpin RNA (shRNA) (sense strand, CCGGTCCGGACTGTCTTAACGCATCATGCACT CGAGTGCATGATGCGTTAAGACAGTTTTTTTG) and three TIP shRNAs (sense strands 1, CCGGTCCGGAGAAGAAGAAGACGCAGCTAGCTCGA GCTAGCTGCGTCTTCTTCTTCTTTTTTTG; 2, CCGGTCCGGCCTGGGA GCAGAGGATGGTCTCTCGAGAGACCATCCTCTGCTCCCAGGT TTTTTG; and 3, CCGGTCCGGGTTTCCTGGTAGCAATGCCACCTCGAG GTGGCATTGCTACCAGGAAACTTTTTTG) were individually cloned at the AgeI and EcoRI sites in the shRNA cassette of Mission pLKO.1-puro vector (Sigma-Aldrich, St. Louis, MO). Three TIP shRNAs were designed to deliver small interfering RNAs (siRNAs) targeting the positions 165 to 185 bp (AGA AGAAGAAGACGCAGCTAG), 466 to 486 bp (CCTGGGAGCAGAGGATG GTCT), and 539 to 559 bp (GTTTCCTGGTAGCAATGCCAC) of the TIP-6 open reading frame. One microgram of the resulting pLKO.1 shRNA plasmid, together with 0.75 μg psPAX2 vector and 0.25 μg pMD2.G vector (Addgene, Inc., Cambridge, MA), was cotransfected into $5 \times 10^5$ HEK-293T cells (Invitrogen) in a six-well plate. After 48 h of incubation at 37°C and 5% $CO_2$, the supernatant was collected and virus particles were concentrated with a PEG-it virus precipitation solution (System Biosciences, Mountain View, CA).

**Recombinant TIPs.** Recombinant TIPs (rTIPs) were generated as glutathione *S*-transferase (GST) fusion proteins GST-TIP-1 to TIP-8 and GST-TIP-6ΔSANT by PCR amplifying the coding regions of TIPs and TIP-6ΔSANT and subcloning them into the pGEX-6P-1 vector (GE Healthcare Biosciences Corp., Piscataway, NJ) between the EcoRI and XhoI ends. All the sequences were verified by sequencing. TIP-1 to TIP-8 and TIP-6ΔSANT were expressed in *Escherichia coli* BL21 (GE Healthcare). GST protein purification was carried out following standard protocols as described previously (2, 40). GST affinity tail was cleaved from TIP-1 to TIP-8 but not from TIP-6ΔSANT or part of TIP-6 using PreScission protease (GE Healthcare). Collected rTIP proteins were concentrated with Microcon filter devices (Millipore, Bedford, MA), resolved by sodium dodecyl sulfate-polyacrylamide gel electrophoresis (SDS-PAGE), and stained by Coomassie blue to verify purity.

**Cell cultures and tissue.** The NIH 3T3 and 3T3-L1 cell lines (American Type Culture Collection) were cultured in Dulbecco's modified Eagle's medium (DMEM) (Invitrogen) supplemented with 10% fetal bovine serum (Invitrogen). Preadipocytes and adipocytes were isolated from the gonadal depots of 5- to 7-day-old mouse pups according to described procedures (58). After 1 h of collagenase digestion (2 mg/ml), the tissue was dispersed and filtered through a 250-μm mesh and centrifuged at $50 \times g$ to eliminate stromal cells for 5 min. The pellet containing vascular and stromal cells was discarded. The infranatant was removed from beneath the floating adipocyte layer and centrifuged at $200 \times g$ for 10 min. The obtained pellet, mainly consisting of preadipocytes, was resuspended and filtered through a 25-μm mesh to remove potential endothelial cell clumps and again sedimented by centrifugation (51). The pellet was resuspended and cultured in advanced DMEM/F12 (Invitrogen) medium supplemented with 10% fetal calf serum (Invitrogen) and 3 μM/ml glucose with 10 μl/ml penicillin (Invitrogen) (58). Simultaneously, floating adipocytes were collected, washed twice in Krebs Ringer's buffer containing 4% albumin, and immediately used for Western blotting. To obtain adipose tissue, the gonadal fat pads from adult mice were removed and rinsed in 0.85% NaCl solution. The fat tissue was then

homogenized in Laemmli buffer with 5% mercaptoethanol and boiled for 10 min. Insoluble material was removed by centrifugation at 14,000 rpm for 15 min.

**Transfections.** NIH 3T3 cells were plated at a density of $2 \times 10^6$ to $3 \times 10^6$ per 100-mm culture dish on the evening before and transfected overnight with empty vector (pcDNA), TIP-1 to TIP-8, and TIP-1ΔSANT to TIP-8ΔSANT (15 μg) using Lipofectamine 2000 (Invitrogen) in Opti-MEM (Invitrogen). To achieve an increased expression of TIP-6ΔSANT, required for some chromatin immunoprecipitation (ChIP) assays, the amount of plasmid transfected was increased by fivefold. Preadipocytes were transfected overnight with empty vector, TIP-1, TIP-1ΔSANT, TIP-3, TIP-3ΔSANT, TIP-6, and TIP-6ΔSANT (15 μg) using Lipofectamine 2000 (Invitrogen) in Opti-MEM, and the cells were allowed to differentiate for 8 to 10 days in culture medium. No chemical adipogenic cocktail was used in these experiments.

**IPs.** Forty-eight hours after transfection, NIH 3T3 cells were lysed in radio IP assay lysis buffer (50 mM Tris, 0.25% deoxycholate, 1% Igepal, 150 mM NaCl, 1 mM EDTA, and 1 mM phenylmethylsulfonyl fluoride) with complete protease inhibitor cocktail tablets (Roche Diagnostics, Indianapolis, IN), precleared with protein A-Sepharose beads (Sigma) and immunoprecipitated with 10 μl of polyclonal x-c-*myc* antibody (Ab) (Sigma) bound to protein A-Sepharose beads (Sigma) overnight at 4°C. The beads were extensively washed with lysis buffer and boiled in Laemmli buffer. The supernatants were then collected after centrifugation. Alternatively, lysates were immunoprecipitated with 10 μl of monoclonal x-p300 Ab, polyclonal x-Tip60 Ab, polyclonal x-CBP Ab (Upstate, Temecula, CA), and x-Gcn5 Ab (Abcam, Inc., Cambridge, MA).

**HAT assay.** HAT activity was measured using a kit from Upstate as described earlier (26). Twenty-five microliters of TIP-1 to TIP-8 and TIP-1ΔSANT to TIP-8ΔSANT IP material or 2 μg of rTIP-1 to TIP-8 were incubated with 100 μM acetyl coenzyme A and 1× HAT assay buffer (50 mM Tris [pH 8.0], 10% glycerol, 0.1 mM EDTA, and 1 mM dithiothreitol) for 30 min on an enzyme-linked immunosorbent assay plate precoated with either biotin-conjugated histone H3 or histone H4 (H3/H4) tail peptides. Acetylated histone was detected colorimetrically at an optical density at 450 nm using an x-acetyl-lysine Ab followed by horseradish peroxidase-conjugated secondary Ab. Twenty nanograms of recombinant PCAF and 10 ng of acetylated H3 and H4 were used as positive controls.

**HDAC assay.** HDAC activity was measured fluorometrically using a kit from Upstate and following the manufacturer's instructions. Twenty-five microliters of TIP IPs were incubated with 60 μl of HDAC assay buffer (25 mM Tris [pH 8.0], 137 mM NaCl, 2.7 mM KCl, and 1 mM $MgCl_2$) containing 100 μM acetylated H3/H4 at 30°C for 45 min. The contents were centrifuged, and 40 μl of the reaction mixture was transferred to a microtiter plate. Twenty microliters of the activator solution was then added, mixed thoroughly, and incubated at room temperature for 15 min. The plate was read in a fluorescence plate reader at excitation at 350 nm and emission at 450 nm. Ten microliters of HeLa cell nuclear extract was used as a positive control.

**HMT assay.** HMT activity was measured using a kit from Upstate. Twenty-five microliters of TIP IPs were incubated with 2 μg of chicken core histones and 0.55 μCi *S*-adenosyl-L-[*methyl*-$^3$H]methionine in HMT assay buffer (50 mM Tris [pH 9.0], 5 mM dithiothreitol) for 30 min at 30°C. Five-microliter aliquots were transferred to the center of 2-cm by 2-cm P81 phosphocellulose papers, and these were washed with 10% trichloroacetic acid followed by 95% ethanol. Radioactive counts were read in a scintillation counter. Two hundred fifty nanograms of purified PRMT1 was used as a positive control.

**Induction of 3T3-L1 adipogenic differentiation.** 3T3-L1 cells were induced to differentiate by the administration of differentiation medium containing DMEM with 10% fetal bovine serum, 10 μg/ml insulin (Sigma), 0.5 mM 3-isobutyl-1-methylxanthine (Sigma), and 1 μM dexamethasone (Sigma) (15, 67). After 48 h, differentiation medium was replaced with regular medium containing 5 μg/ml insulin (15, 67). The culture medium was changed at 2-day intervals. The cells were used for different studies at 0, 1, 2, 3, 4, 5, and 10 days after induction.

**3T3-L1 cell stretching.** In some experiments, 3T3-L1 cells were statically stretched for 6 h as previously described (26, 59) starting after 18 h of induction. The cells were then collected for studying TIP expression.

**Lentivirus infection.** The viral supernatants ($3.3 \times 10^8$) were used to infect the 3T3-L1 cells. The cells were treated with Polybrene (8 μg/ml) (Sigma) for 30 min before incubating with control (scrambled) lentivirus and TIP-targeting lentivirus overnight, and subsequently, the cells were maintained in the medium containing puromycin for 1 week to select cell populations stably infected with the viruses. The infected cells were induced with differentiation medium.

**p300 and Gcn5 RNA interference.** NIH 3T3 cells were cultured in 100-mm plates to 70% confluence. Twenty micromolar siGenome SMART pool p300, Gcn5, or scrambled siRNA (Dharmacon, Lafayette, CO) and 2 μM siGLO RISC-free transfection efficiency control siRNA (Dharmacon) were simultaneously transfected with 15 μg of empty vector, TIP-6, or TIP-6ΔSANT using FuGENE 6 (Roche Diagnostics) following the manufacturer's protocol for 76 h. Decreases in the p300 and Gcn5 levels were determined by Western blotting.

**Western blots.** Fifty micrograms of fat lysates, 60 μg of cell lysates of 3T3-L1 cells differentiated for 0, 1, 2, 3, 4, 5, and 10 days or lentivirus-infected 3T3-L1 cells differentiated for different days, and 25 μl of x-myc, x-p300, x-Tip60, x-Gcn5, and x-CBP IPs of NIH 3T3-transfected cells were boiled in Laemmli buffer with 5% mercaptoethanol, resolved on 4 to 12% SDS-PAGE gels, and transferred onto nitrocellulose membranes (Bio-Rad Laboratories, Hercules, CA). The membranes were blocked with 3% milk and probed with polyclonal x-TIP Ab (26), x-myc Ab, x-p300 Ab, x-Tip60 Ab, x-Gcn5 Ab, x-CBP Ab, monoclonal x-histone H3 Ab (Upstate), or monoclonal x-histone H4 Ab (Abcam). All these primary Abs were used at a 1:1,000 dilution and detected with horseradish peroxidase-conjugated secondary Abs diluted 1:10,000. The bands were visualized with the ECL chemiluminescence kit from GE Healthcare.

**Reverse transcriptase PCR (RT-PCR).** Total RNA was extracted with TRIzol (Invitrogen) from fat; NIH 3T3 cells transfected with empty vector, TIP-6, and TIP-6ΔSANT; and 3T3-L1 cells induced and noninduced. cDNA was then synthesized using the iScript cDNA synthesis kit (Bio-Rad Laboratories, Hercules, CA). The primers used in this study included the following: GAPDH (glyceraldehyde-3-phosphate dehydrogenase) sense, 5′-ATCACCATCTTCCAGGAGCGA-3′, and antisense, 5′-GCCAGTGAGCTTCCCGTTCA-3′; PPARγ2 sense, 5′-CCCTGATGAATAAAGATGGA-3′, and antisense, 5′-GAGGTCTGTCATCTTCTGGA-3′; adipsin sense, 5′-TCTATACCCGAGTGTCATCC-3′, and antisense, 5′-GATGGCTCAGTGGTTAAGAG-3′; adipocyte protein (aP-2) sense, 5′-TCTCCAGTGAAAACTTCGAT-3′, and antisense, 5′-GAAGTCACGCCTTTCATAAC-3′; C/EBPα sense, 5′-AGGTGCTGGAGTTGACCAGT-3′, and antisense, 5′-CAGCCTAGAGATCCAGCGAC-3′ (26); C/EBPβ sense, 5′-CTATTTCTATGAGAAAAGAGGCGTATGTAT-3′, and antisense, 5′-ATTCTCCCAAAAAAGTTTATTAAAATGTCT-3′; C/EBPδ sense, 5′-TGCCCACCCTAGAGCTGTG-3′, and antisense, 5′-CGCTTTGTGGTTGCTGTTGA-3′; leptin sense, 5′-GATCAATGACATTTCACACA-3′, and antisense, 5′-GGACGCCATCCAGGCTCTCT-3′; and KLF5 sense, 5′-CCGGAGACGATCTGAAACAC-3′, and antisense, 5′-GGAGCTGAGGGGTCAGATACTT-3′. TIPs expression was detected using the following primer sets: TIP-1 sense, 5′-CAAGAATCGTAATTGGCTGTTGAG-3′, and antisense, 5′-GGATCCTGGAATGTTCCTCTAGTATTC-3′; TIP-2 sense, 5′-CCTTTCTCTACTGCTGCGACT-3′, and antisense, 5′-GCAGGTCTGTACCCTCTTCCT-3′; TIP-3 sense, 5′-CCAAAGGTCCTGCTTAGGATG-3′, and antisense, 5′-TCCCGAAACAATAGCATTCC-3′; TIP-4 and TIP-5 sense, 5′-CTTTGTATTTTCCTGCCATCAAG-3′, and antisense, 5′-ACAGCCAATTACGATTCTTG-3′; TIP-6 sense, 5′-ATCATCCTGGGATCAAGTCG-3′, and antisense, 5′-CTCTCATACAGTACCTCTAGTATTCG-3′; TIP-7 sense, 5′-CTCCAGAAGAGCAAGAACCTG-3′, and antisense, 5′-CCATGTCTGACGCTAAGCAA-3′; and TIP-8 sense, 5′-CAAGAATCGTAATTGGCTGTTGAG-3′, and antisense, 5′-GAAAACACTTAAAACTCACTGCAAG-3′. All amplifications were run for 35 cycles. The amplified PCR products were visualized on 1% agarose gels using 0.5 μg/ml ethidium bromide. Amplicons were confirmed by sequencing.

**Real-time PCR.** Total RNA was extracted and cDNA was synthesized as mentioned above from fat; NIH 3T3 cells transfected with empty vector, TIP-6, and TIP-6ΔSANT; 3T3-L1 cells; and lentivirus-infected 3T3-L1 cells induced with standard differentiation medium for different days. cDNA was amplified and detected with the FullVelocity Sybr green QPCR master mix (Stratagene) according to the manufacturer's protocol. The PCR primers were the same as those used for the semiquantitative RT-PCR. The real-time PCR was carried out in Mx4000 Multiplex quantitative PCR systems (Stratagene), and its software was used to calculate the cycle threshold.

**Promoter-reporter assay.** Promoter-reporter constructs were made for different PPARγ2 promoter (AY243584) fragments in the forward direction, from positions −1140 to +52 bp referred to as full-length (PPARγ2p.FL or FL), −631 to +52 bp (M1), −361 to +52 bp (M2), and −631 to −361 bp (M3) using the following respective primer sets: sense, 5′-AAGCTTGACAGAGAACTCTTGCTAGTCCC-3′, and antisense, 5′-AAGCTTCAGAGATTTGCTGTAATTCACACTG-3′; sense, 5′-AAGCTTCTGTCAACTATTCCTTTTTATAGAATTTGG-3′, and antisense, 5′-AAGCTTCAGAGATTTGCTGTAATTCACACTG-3′; sense, 5′-AAGCTTGCCACTGGTGTGTATTTTACTGC-3′, and antisense, 5′-AAGCTTCAGAGATTTGCTGTAATTCACACTG-3′; and sense, 5′-AAGCTTCTGTCAACTATTCCTTTTTATAGAATTTGG-3′, and antisense, 5′-AAGCTTGTAAAATACACACCAGTGGCTTTTAA-3′. The resulting PCR products were cloned into the HindIII site of the firefly luciferase reporter vector pGL3. The C/EBP binding site (−340 to −322) and KLF binding site (−278 to −267) deletion mutant reporter constructs (M4 and M5, respectively) were made using a QuikChange II site-directed mutagenesis kit (Stratagene).

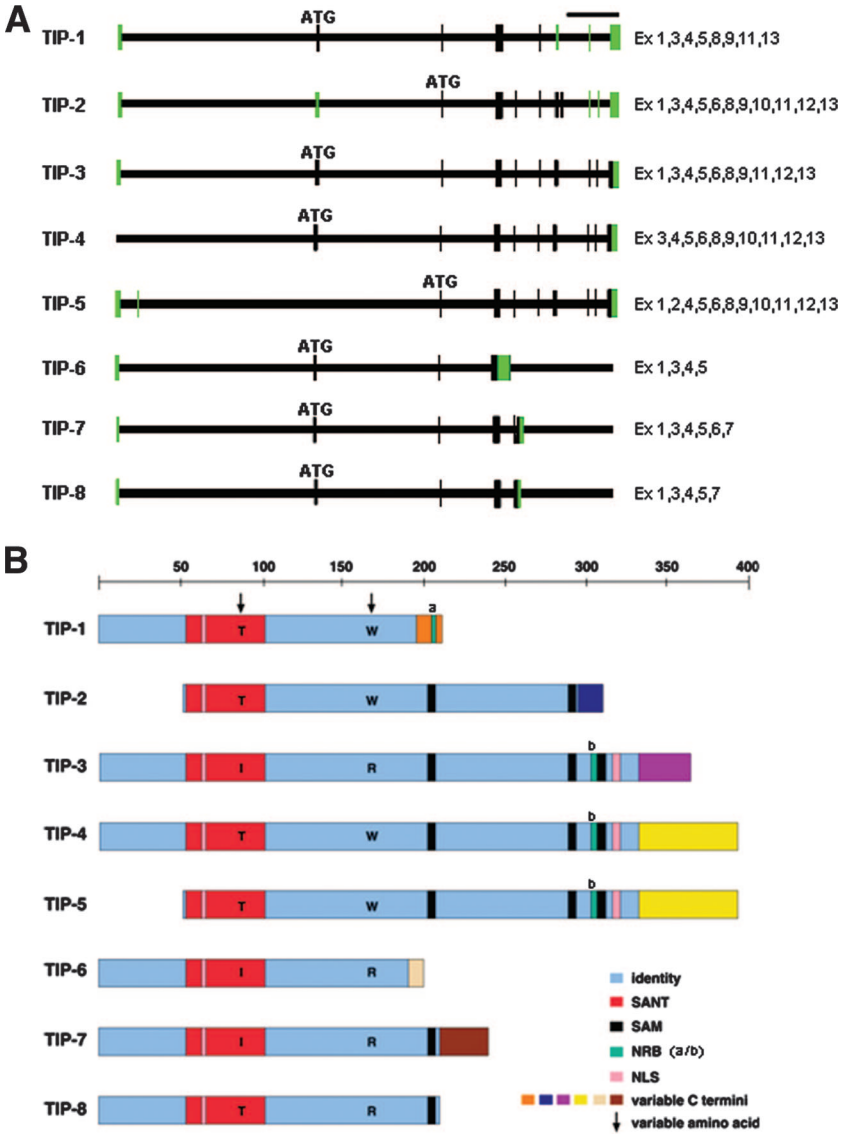


FIG. 1. (A) Schematic map of the mouse *tip* gene. Coding (black) and noncoding (green) exons are shown as vertical boxes. The exon composition of each isoform is listed to the right. The initiation codon (ATG) is also shown. A 10-kb scale is included at the top right corner of the map. (B) Schematic representation of the eight TIP isoforms. TIP-2 and TIP-5 lack the first 51 amino acids common to all the others. The amino acids at position 162 are W in TIP-1, TIP-2, TIP-4, and TIP-5 and R in TIP-3, TIP-6, TIP-7, and TIP-8. All TIPs have nuclear localization signals or NLS (pink) and SANT domains (red). Six TIPs have SAM domains (black); TIP-3, TIP-4, and TIP-5 have three SAM domains; TIP-2 has two; and TIP-7 and TIP-8 have one. TIP isoforms without SAM domains are TIP-1 and TIP-6. TIP-1, TIP-3, TIP-4, and TIP-5 have NRBs (green). TIP-1 has NRBa (labeled "a" above the box) and the other three have NRBb (labeled "b" above the box). TIP-1 to TIP-7 also have a variable amino acid region in their C termini (various colors) which is unique to each TIP except for TIP-4 and TIP-5, which have identical C-terminal regions.

TIP-6 and TIP-6ΔSANT (4.5 μg) were transfected simultaneously with 50 ng of firefly luciferase reporter plasmid containing full-length PPARγ2 promoter (PPARγ2p.FL) and 5 ng of *Renilla* luciferase plasmid (pRL-TK from Promega Corporation, Madison, WI) to normalize the transfections. In additional experiments, 4.5 μg of TIP-6 was transfected simultaneously with 50 ng of full-length PPARγ2 promoter (FL) or its deletion mutant reporter constructs (M2 to M5) and 5 ng of pRL-TK. The transfection of empty vector with PPARγ2p.FL served as the control (mock). Cell extracts were prepared 48 h after transfection and assayed for firefly and *Renilla* luciferase activities using the dual-luciferase promoter-reporter assay kit from Promega as per the manufacturer's instructions. pGL3 empty control (pGL3 basic) values were considered baseline values and were therefore subtracted from all three groups.

**Oil Red O staining.** This was performed as described earlier (26). Ten-day-posttransfection preadipocyte cultures and 3T3-L1 cells were stained with Oil Red O in propylene glycol (Poly Scientific R&D Corp., Bay Shore, NY) for 30 min at 37°C, washed with water, air dried, and counterstained with hematoxylin. For the quantification of cells, Oil Red O staining was performed on trypsinized cells in suspension, and cells positive and negative for Oil Red O staining were then counted using a hemocytometer.

**GST pull-down assay.** GST alone, GST-TIP-6, and GST-TIP-6ΔSANT were immobilized onto glutathione Sepharose 4B beads (GE Healthcare), and these were incubated overnight at 4°C with 2 μg of purified H4 (Upstate) or recombinant p300 (produced in insect cells; Active Motif, Carlsbad, CA) in binding buffer (10 mM Tris at pH 8.0, 150 mM NaCl, 1 mM $MgCl_2$, 0.5% Triton X-100,

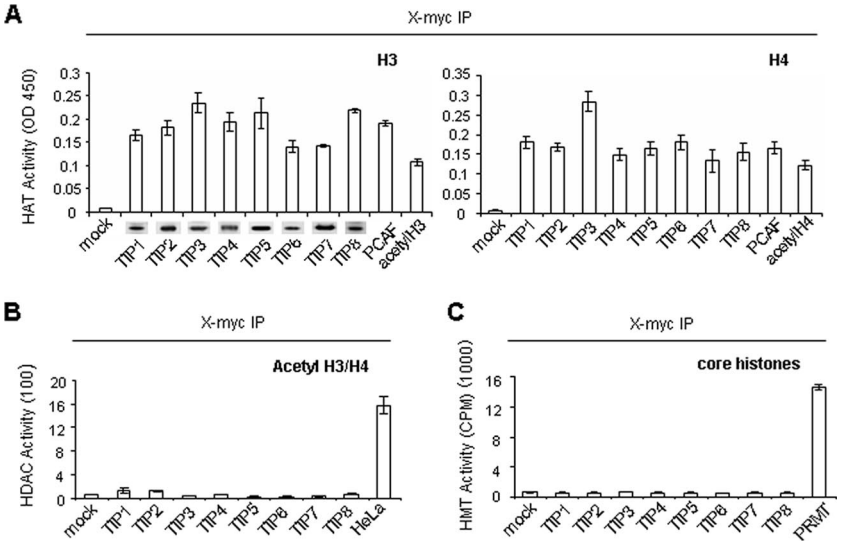


FIG. 2. (A) TIP IPs have HAT activity. myc-tagged TIPs (TIP1 to TIP8) and empty vector (mock) were expressed in NIH 3T3 cells, and x-myc IPs were used to perform HAT assays on H3 and H4 substrata. All the IPs have HAT activity for both substrata. The histogram of HAT activity on H3 includes immunoblots demonstrating the presence of transfected TIPs in the IP material. The HAT PCAF and acetyl H3/H4 are included as positive controls. The error bars on top of each column represent the standard errors. OD450, optical density at 450 nm. (B and C) No HDAC (B) or HMT (C) activity is observed in TIP IPs on acetyl H3/H4 and nucleosome substrata, respectively. HeLa cell nuclear extracts and the HMT PRMT are, respectively, included as positive controls for HDAC and HMT activity assays. The error bars on top of each column represent the standard errors. The results are representative of three experiments, each performed in triplicate.

10% glycerol, 1 mM dithiothreitol) (40). After extensive washing, the beads were suspended in Laemmli buffer with 5% mercaptoethanol and boiled for 5 min, and 30 μl of supernatant was resolved by SDS-PAGE and transferred to nitrocellulose membranes. The samples were analyzed by Western blotting using x-TIP, x-H4, and x-p300 Abs at the concentrations stated above.

**ChIP assays.** ChIP assays were conducted with NIH 3T3 cells transfected with empty vector, TIP-6, and TIP-6ΔSANT and 3T3-L1 cells induced for 0 days or 10 days as previously described (26) using a ChIP assay kit from Upstate. Six micrograms of x-TIP; x-myc; x-p300; x-Gcn5; polyclonal x-acetylhistone H3K9,14 (Upstate); polyclonal x-acetylhistone H4K5,8,12,16 (Upstate); and polyclonal x-acetylhistone H4K16 Abs (Upstate) and 10 μl of monoclonal x-RNA polymerase II Ab and clone 8WG16 (Upstate) were used for the IPs. An aliquot of chromatin DNA prepared from cell lysates taken prior to the IP was considered as input DNA. The IP DNA and input DNA were analyzed by PCR. The primer pairs used were 5′-GCCACTGGTGTGTATTTTAC-3′ (−361 to −342) and 5′-CAAATATTTGGGAGAGGTGGG-3′ (−93 to −73) for the PPARγ2 gene promoter (26) and 5′-TGACTTAGAGGCTTAAAGGA-3′ (−315 to −296) and 5′-CGGGGACCGCTTTTATAGAG-3′ (−37 to −18) for the C/EBPα gene promoter (45). The amplified PCR products were visualized on 1% agarose gels using 0.5 μg/ml ethidium bromide and quantified by real-time PCR.

## RESULTS

**The TIP family is currently composed of eight isoforms.** In addition to the three TIPs originally identified, a GenBank search indicated the existence of three additional TIP isoforms (TIP-5, TIP-6, and TIP-7). TIP-4 and TIP-8 were identified in C3H/10T1/2 multipotential mesenchymal cells (64) while cloning TIP-5 and TIP-7. These eight isoforms are generated by alternative splicing from a single gene located in chromosome 2q22-23 in mice and 2q31.1 in humans. The exon composition of each TIP is presented in Fig. 1A. Their predicted molecular masses are 24, 28.5, 40.5, 44.5, 38.5, 22.5, 27, and 24 kDa, respectively. Figure 1B shows a schematic representation of the eight isoforms. TIP-2 and TIP-5 lack the first 51 amino acids common to all the others. The amino acids at position 162 are W in TIP-1, TIP-2, TIP-4, and TIP-5 and R in TIP-3, TIP-6, TIP-7, and TIP-8. All TIPs have NLS (pink) and SANT domains (red). In addition, six TIPs have SAM domains (black); TIP-3, TIP-4, and TIP-5 have three SAM domains; TIP-2 has two; and TIP-7 and TIP-8 have one. The isoforms without SAM domains are TIP-1 and TIP-6. TIP-1, TIP-3, TIP-4, and TIP-5 have NRBs (green). TIP-1 has NRBa (LSLLL), and the other three have NRBb (LSRLL). TIP-1 to TIP-7 also have a variable amino acid region in their C termini (various colors) which is unique to each TIP except for TIP-4 and TIP-5, which have identical C-terminal regions.

**TIP IPs have HAT activity.** Since all TIPs have structural domains characteristic of histone-modifying enzymatic complexes with HAT, HDAC, or HMT activity, we tested them for each of these activities. TIPs tagged with myc were expressed in NIH 3T3 cells, which have no endogenous TIP expression, and the IPs generated with an x-c-*myc* Ab were used to perform HAT, HDAC, and HMT assays. We found that all the IPs had HAT activity on H3 and H4 substrata (Fig. 2A). Immunoblots confirmed the presence of TIP isoforms in each IP (Fig. 2A). No HDAC or HMT activity was observed on acetylated H3/H4 or core histones, respectively (Fig. 2B and C).

**TIPs recruit p300 HAT activity.** Since SANT, SAM, and NRB are found in both catalytic and noncatalytic subunits within histone-modifying enzymatic complexes, we next performed HAT assays using rTIPs on H3 and H4 substrata to determine whether TIPs have intrinsic catalytic activity. rTIPs did not have HAT activity on either substrata (Fig. 3A), indicating that the catalytic activity present in the IPs was the result of a recruited HAT enzyme(s). To identify a TIP-associated HAT enzyme(s), we performed Western blotting using x-myc IPs from TIP-1 to TIP-8 NIH 3T3 transfected cells using Abs against various HAT enzymes. These showed that all TIPs coimmunoprecipitate the HAT p300 enzyme (Fig. 3B). No

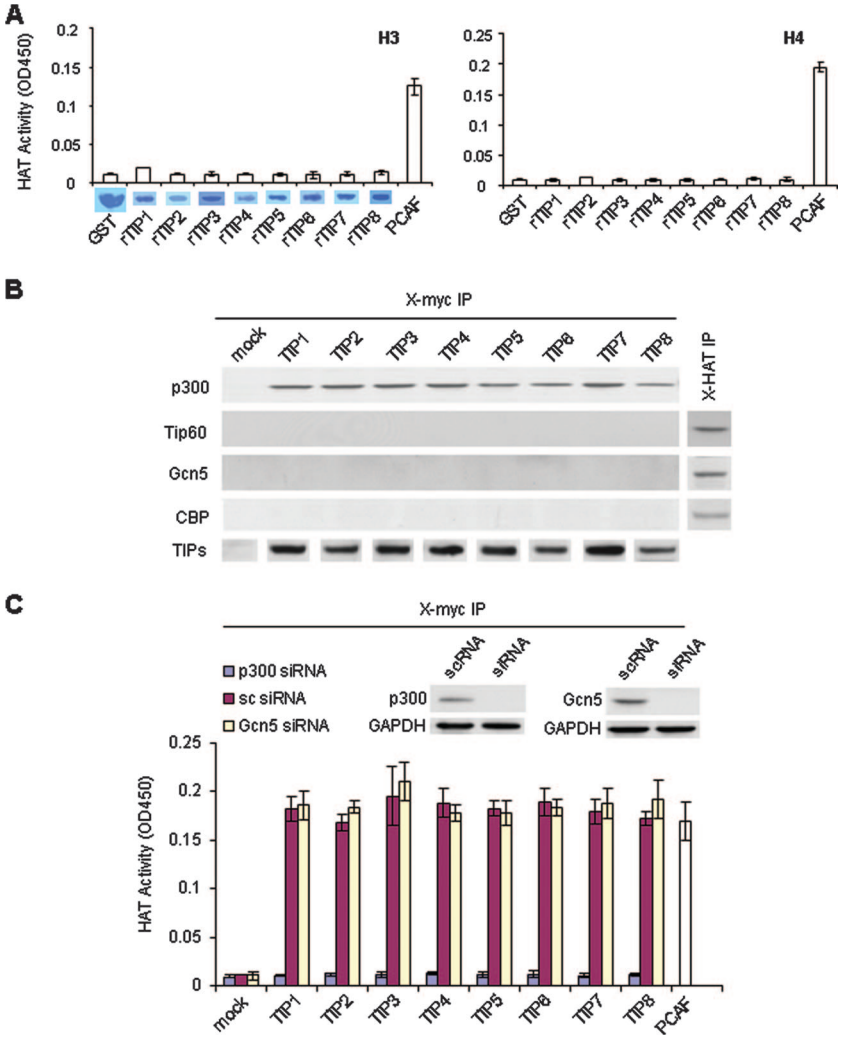


FIG. 3. TIPs recruit p300 HAT activity. (A) rTIPs generated as GST fusion proteins were used to perform HAT assays on H3 and H4 substrata after removing the GST peptide. None of the rTIPs have intrinsic HAT activity on either substratum. The histogram of HAT activity on H3 includes Coomassie blue staining of rTIPs and GST (negative control). The error bars on top of each column represent the standard errors. (B) TIPs coimmunoprecipitate the HAT enzyme p300. myc-tagged TIPs (TIP1 to TIP8) and empty vector (mock) were expressed in NIH 3T3 cells, and x-myc IPs were analyzed by Western blotting with antibodies against various HATs. p300, but no other HATs, was detected in all IPs. x-myc immunoblots demonstrate the presence of transfected TIPs in the IP material. IPs with x-Tip60, x-Gcn5, and x-CBP Abs (X-HAT IP) followed by immunoblotting with the same Abs demonstrated the presence of these HATs in NIH 3T3 cells. (C) p300 silencing inhibits TIP-recruited HAT activity. myc-tagged TIPs (TIP1 to TIP8) and empty vector (mock) were expressed in NIH 3T3 cells in which p300 was suppressed by RNAi. There is a significant decrease in HAT activity in cells treated with a p300 siRNA probe (blue columns) compared to that in cells treated with the scrambled RNA (scRNA) control probe (red columns). The suppression of Gcn5 does not affect TIP-recruited HAT activity (yellow columns). The HAT PCAF is included as a positive control. The error bars on top of each column represent the standard errors. The Western blots included with the histogram demonstrate no p300 in cells treated with the p300 and Gcn5 siRNA probes compared with the scRNA probes. GAPDH is shown as a loading control. The results are representative of three experiments. The experiments depicted in panels A and C were performed in triplicate. OD450, optical density at 450 nm.

other HATs tested, including Tip60, Gcn5, and CBP, were found in the IPs (Fig. 3B). IPs with x-Tip60, x-Gcn5, and x-CBP Abs followed by immunoblotting with the same Abs demonstrated the presence of these HATs in NIH 3T3 cells (Fig. 3B). To determine whether p300 was responsible for the recruited TIP HAT activity, we conducted HAT assays using x-myc IPs from TIP-transfected cells in which p300 or Gcn5 production was suppressed using siRNA probes. The suppression of p300 eliminated HAT activity, whereas the suppression of Gcn5 had no effect (Fig. 3C).

**Deletion of the SANT domain inhibits TIP-recruited HAT activity.** Figure 4A shows the alignment of the TIPs SANT domain with SANT domains found in other histone-modifying enzymatic complexes. The conserved bulky aromatic residues are boxed in black. The TIP SANT domain is closest in homology to the N-CoR SANT domain, which is 20% identical and 46% similar (Fig. 4A). As other previously reported SANT domains, TIP SANT domains have a theoretical isoelectric point of 5, which makes binding to DNA highly unlikely due to its negative electrostatic surface potential, as predicted by

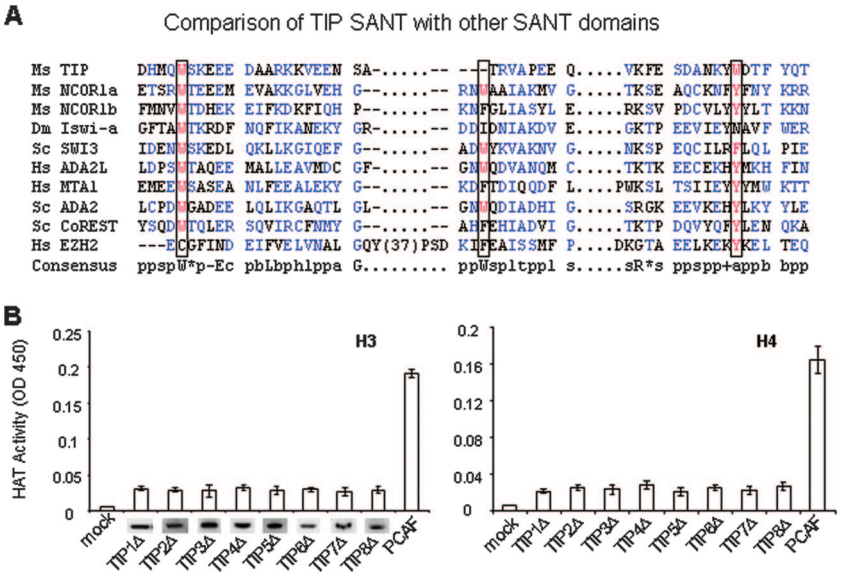


FIG. 4. The SANT domain is required for TIP-recruited HAT activity. (A) TIP SANT domains compared with SANT domains present in other histone-modifying enzymatic complexes (using the SMART program). The conserved bulky aromatic residues are boxed in black. The TIP SANT domain has the closest homology to the N-CoR SANT, which is 20% identical and 46% similar with it. The conserved bulky aromatic residues in the TIP SANT domain have a theoretical isoelectric point of 5. (B) TIP mutants with a SANT deletion (TIP1Δ to TIP8Δ) and empty vector (mock) were expressed in NIH 3T3 cells, and x-myc IPs were used for HAT assays. These show significant reduction in HAT activity on H3 and H4 (compare to wild type in Fig. 2A). The histogram of HAT activity on H3 includes immunoblots demonstrating the presence of transfected TIPΔSANT isoforms in the IP material. The HAT PCAF is included as a positive control. The error bars on top of each column represent the standard errors. The results shown are representative of three experiments performed in triplicate.

structural modeling (11). Since SANT domains have been previously shown to be involved in H3/H4 acetylation, we transfected TIPΔSANT mutants into NIH 3T3 cells and performed HAT assays with the TIPΔSANT IPs. The deletion of the SANT domain drastically inhibited HAT activity on the H3 and H4 substrata (Fig. 4B).

**TIP-6 is present in mature adipose tissue and induces PPARγ2-mediated adipogenesis.** To study the functional role of the SANT domain in more depth, we focused further studies on TIP-6, the shortest TIP and the only one with a $SANT^+$ $SAM^-$ $NRB^-$ makeup. We first determined whether TIP-6 transfection could induce differentiation in NIH 3T3 cells. TIP-6 indeed promoted adipogenic gene expression. This was indicated by the de novo induction of the key adipogenic nuclear receptor/transcription factor PPARγ2, downstream adipogenic transcription factor C/EBPα, and terminal differentiation markers adipsin and aP-2, as demonstrated by RT-PCR and real-time PCR (Fig. 5A and B, respectively). The effect of TIP-6 was only partial, as it did not induce leptin, another marker of adipocyte terminal differentiation (Fig. 5A and B), or result in the intracellular accumulation of lipids even after treatment with chemical adipogenic inducers (K. R. Badri and L. Schuger, unpublished data). Unlike TIP-6, TIP-6ΔSANT did not induce adipogenic genes (Fig. 5A and B). C/EBPβ and C/EBPδ, which act upstream of PPARγ2, were not induced by TIP-6 (Fig. 5A and B) (data not shown). Markers of myogenic differentiation were not observed (data not shown).

Promoter-reporter assays were performed using a pGL3 PPARγ2 promoter construct transfected into NIH 3T3 cells along with TIP-6 or TIP-6ΔSANT or empty vector. These studies showed that TIP-6 activated the PPARγ2 promoter and that activation was eliminated by the deletion of the SANT domain (Fig. 5C). Promoter deletion studies further showed that a bp −361 to +52 PPARγ2 promoter fragment was sufficient to substitute for the full PPARγ2 promoter in the TIP-6-induced luciferase expression assays (Fig. 5D and E). Its activity did not change by deleting either the C/EBP binding sites (41, 66) or the KLF binding site (41) (Fig. 5D and E).

To further test the role of TIP-6 in adipogenesis, we transfected TIP-6 or TIP-6ΔSANT into preadipocytes in primary culture, in which endogenous TIP-6 was not detected by immunoblotting (data not shown). TIP-6 had a dramatic effect on preadipocytes, rapidly inducing their differentiation into mature adipose cells as indicated by the large accumulation of intracellular lipids stained red with Oil Red O (Fig. 6A). TIP-6ΔSANT did not induce differentiation (Fig. 6A). The quantification of fat-positive cells in preadipocyte primary cultures transfected with TIP-6 as well as TIP-1 (myogenic), TIP-3 (adipogenic), and their respective SANT-deleted mutants is presented in Fig. 6B, which shows adipogenic differentiation after TIP-3 or TIP-6 transfection and lack of adipogenic differentiation upon transfection with TIP-1 or TIPΔSANT mutants. Equally important, TIP-6, along with TIP-3, was identified by RT-PCR and immunoblotting of the fat of adult mice (Fig. 6C to E). Immunoblots of freshly isolated mature adipose cells, which unlike intact fat do not contain additional cell types, such as vascular and stromal cells, also showed restricted TIP-3 and TIP-6 presence (not shown).

We next determined whether adipogenic TIP-1 and TIP-3 and/or other TIP isoforms are expressed during 3T3-L1 adipogenic differentiation. No TIP message was detected in non-induced 3T3-L1 cells, and only TIP-6 mRNA was detected

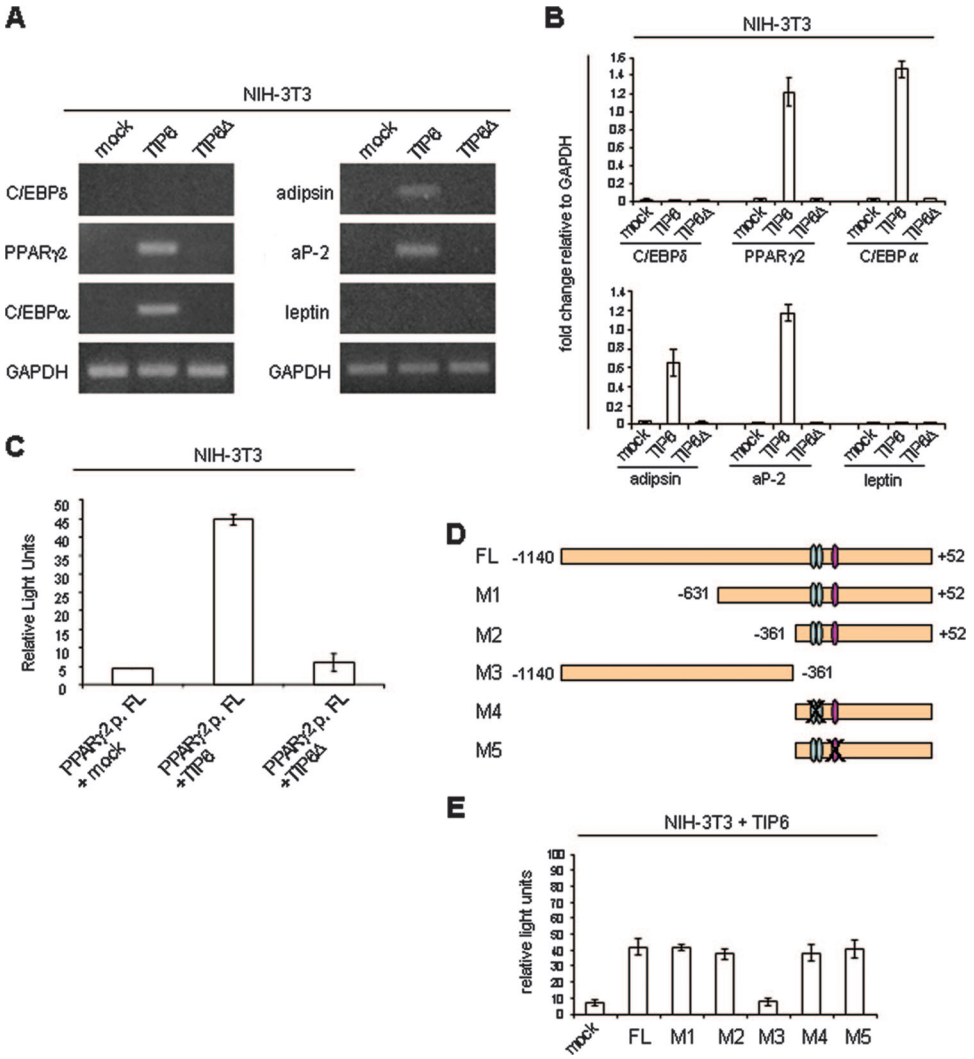


FIG. 5. TIP-6 induces adipogenic gene expression by activating PPARγ2 promoter-mediated transcription. (A and B) TIP-6 promotes adipogenic gene expression in NIH 3T3 cells. TIP-6 (TIP6), TIP-6ΔSANT (TIP6Δ), and empty vector (mock) were transfected into NIH 3T3 cells, and the cells were examined for adipogenic markers by RT-PCR (A) and real-time PCR (B) 48 h after transfection. The TIP-6 induction of adipogenic gene expression is indicated by the de novo induction of the nuclear receptor/transcription factor PPARγ2, downstream adipogenic transcription factor C/EBPα, and terminal differentiation markers adipsin and aP-2. TIP-6 does not induce leptin, another marker of adipocyte terminal differentiation. C/EBPδ, acting upstream of PPARγ2, is not induced by TIP-6. As a control for the RT-PCR, GAPDH is equally amplified in all samples. (C) TIP-6 activates PPARγ2 promoter-mediated transcription. The dual-luciferase promoter-reporter assay performed with NIH 3T3 cells cotransfected with the PPARγ2 full-length promoter-reporter construct (PPARγ2p.FL) and either empty vector (mock), TIP-6 (PPARγ2p.FL + TIP6), or TIP-6ΔSANT (PPARγ2p.FL + TIP6Δ) showed TIP-6-mediated activation of the PPARγ2 promoter. Activation is eliminated by the deletion of the SANT domain. Transfections were normalized with *Renilla* luciferase. (D and E) A −361 to +52 PPARγ2 promoter fragment is sufficient for the full TIP-6 activation of PPARγ2 promoter-mediated transcription. Panel D shows the full PPARγ2 promoter (FL) and the deletions tested (M1 to M5). The blue bars represent the C/EBP binding sites, and the pink bar represents the KLF binding site. (E) Dual-luciferase promoter-reporter assay performed with NIH 3T3 cells cotransfected with TIP-6 and the various PPARγ2 promoter-reporter deletion constructs or vector alone (mock). A fragment comprising bp −361 to +52 (M2, M4, and M5) activates transcription to a degree similar to the full-length promoter (FL). The deletion of either the C/EBP or KLF binding sites does not affect transcription (M4 and M5). No transcription is observed with a fragment encompassing bp −1140 to −361 (M3). The transfections were normalized with *Renilla* luciferase. The error bars on top of each column represent the standard errors in panels B, C, and D. The results shown are representative of three experiments.

after adipogenic induction was completed (Fig. 7A). These results were confirmed by real-time PCR (not shown). Kinetic studies using real-time PCR and Western blotting confirmed the absence of TIP-6 mRNA and protein at time zero (Fig. 7B and C). Increased levels of TIP-6 message and incipient TIP-6 protein production were already detected 24 h after adipogenic induction (Fig. 7B and C), reached a peak around day 5, and continued to be detected, albeit at lower levels, during the rest of the 10-day culture period (Fig. 7B and C). TIP-3 was not induced in this in vitro adipogenic model (Fig. 7A to C). Six hours of continuous stretching starting 18 h after the addition of the adipogenic cocktail suppressed the incipient TIP-6 message and protein production seen at 24 h after adipogenic induction (not shown). Figure 7D shows the time-course ex-

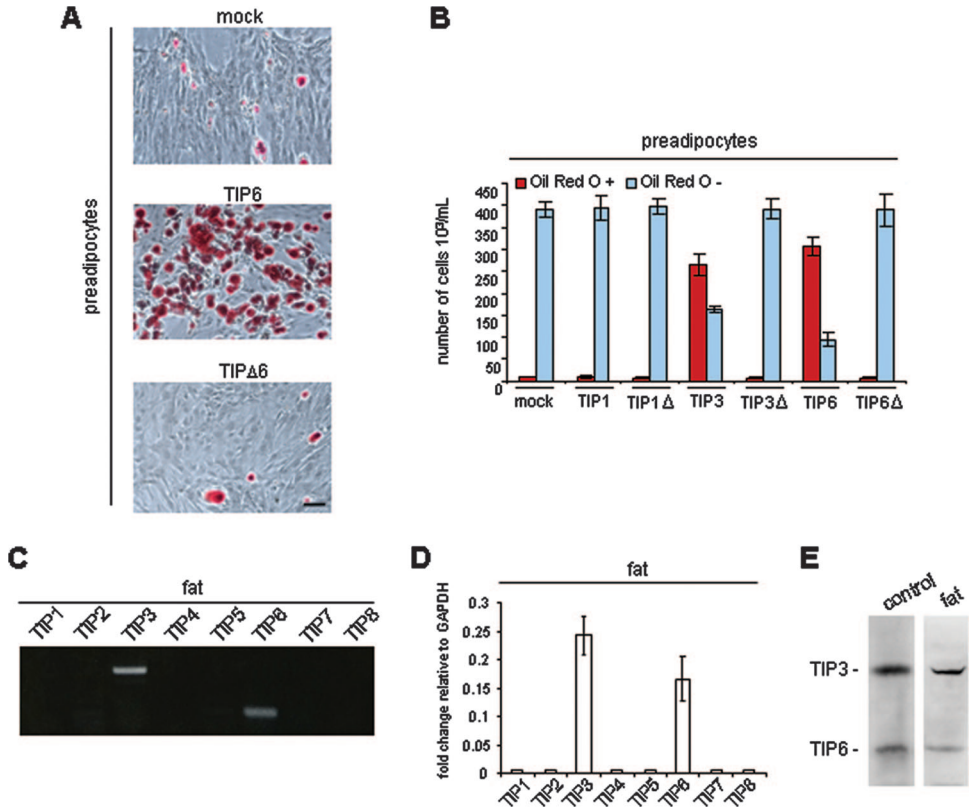


FIG. 6. TIP-6 induces preadipocyte maturation in vitro and is present in mature adipose tissue in vivo. (A) TIP-6 induces preadipocytes to differentiate into mature adipose cells. TIP-6 (TIP6), TIP-6ΔSANT (TIP6ΔSANT), and empty vector (mock) were transfected into mouse preadipocytes in primary cultures and stained with Oil Red O 10 days after transfection to detect the presence of fat (red). Abundant fat accumulation is seen in TIP-6-transfected cells. A few fat-laden cells are also detected in the mock- and TIP-6ΔSANT-transfected cells. Scale bar = 50 μm. (B) Quantification of fat-positive cells in preadipocyte primary cultures transfected with TIP-6 as well as TIP-1 (myogenic), TIP-3 (adipogenic), and their SANT-deleted mutants. A few fat-positive cells are seen in the mock-, TIP-1-, and TIPΔSANT-mutant-transfected cells (red column), whereas cells transfected with TIP-3 and TIP-6 present numerous fat-positive cells. The blue columns represent the number of fat-negative cells. (C to E) TIP-6 and TIP-3 transcripts (C and D) and protein (E) in mature mouse adipose tissue, identified by RT-PCR and Western blotting, respectively. The control for the immunoblot bands represents NIH 3T3 cells cotransfected with TIP-3 and TIP-6. The error bars on top of each column represent the standard errors (B and D). The results shown in panels A to D are representative of three experiments.

pression of C/EBPβ, PPARγ2, and C/EBPα, which are normally induced during 3T3-L1 adipogenic differentiation (15, 41, 45, 55). Two other adipogenic transcription factors, CEBPδ and KLF5, and the fat specific protein aP-2 were tested and showed a similar pattern of expression as previously published (27, 41, 45) (not shown). The inhibition of TIP-6 production by RNA interference (RNAi) significantly inhibited 3T3-L1 adipogenic differentiation, as indicated by the inhibition of PPARγ2 and C/EBPα gene expression (Fig. 7E) and by a marked decrease in fat-positive cells (Fig. 7F and G). C/EBPβ, which was not induced by TIP-6 expression in NIH 3T3 cells, was not inhibited by silencing TIP-6 (Fig. 7E). Studies performed on days 0, 1, 2, 3, 4, 5, and 10 confirmed that TIP-6 mRNA and protein were suppressed during the entire RNAi treatment (Fig. 7E) (data not shown).

**TIP-6 binds directly and indirectly to p300 and H4. Direct TIP-6-p300 binding is SANT mediated.** Since the SANT domains in noncatalytic subunits of histone-modifying complexes (such as is the case for TIPs) have been shown to interact with H3/H4 and/or with the catalytic subunit, we studied TIP-6 and TIP-6ΔSANT IPs for the presence of p300, H3, and H4. As expected, TIP-6 coimmunoprecipitates p300; in addition, TIP-6 coimmunoprecipitates H4, but H3 was not detected. TIPΔSANT also coimmunoprecipitates p300 and H4, but the p300 levels were lower (approximately 50% by immunoblot densitometry) than those present in TIP-6 IPs (Fig. 8A). IPs using an x-p300 Ab confirmed these co-IP results and demonstrated that in the absence of TIP-6, p300 does not interact with H4 (Fig. 8B). GST pull-downs using the GST-TIP-6 and GST-TIP-6ΔSANT fusion proteins, recombinant p300, and purified H4 showed the direct binding of TIP-6 to p300 and H4 (Fig. 8C). TIP-6-H4 binding was not affected by SANT domain deletion (Fig. 8C). The binding of TIP-6 to p300 was, however, eliminated by deleting the SANT domain (Fig. 8C). Since TIP-6ΔSANT coimmunoprecipitates p300, our results indicated that TIP-6 binds to p300 not only directly but also indirectly through other yet-uncharacterized protein(s) complexing with TIP-6 and p300.

**TIP-6 and TIP-6ΔSANT are recruited to the PPARγ2 promoter but only TIP-6 allows for p300-mediated promoter-associated H3/H4 acetylation.** To further determine how TIP-6 induces adipogenesis, we transfected TIP-6 and TIP-6ΔSANT

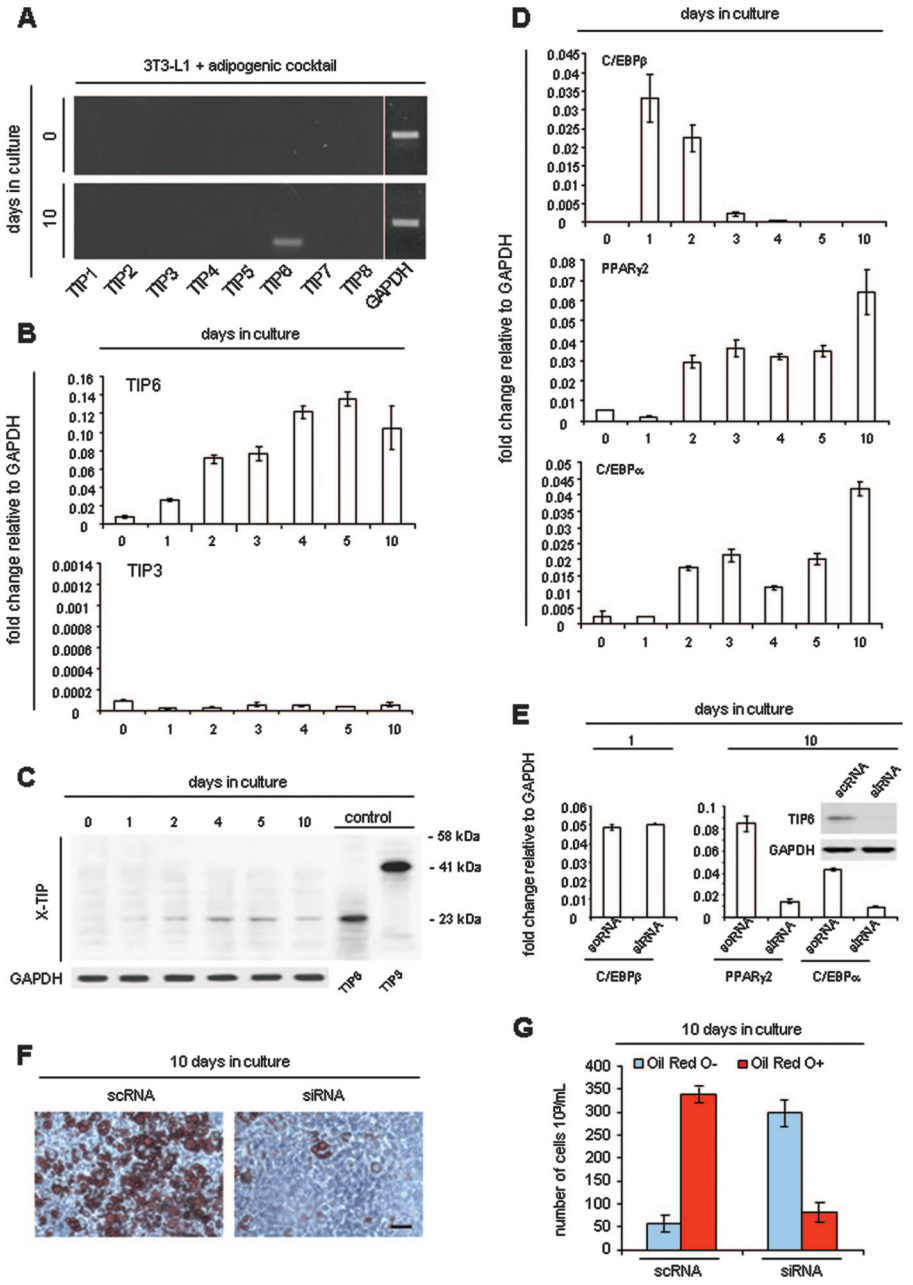


FIG. 7. TIP-6 is induced during the adipogenic differentiation of 3T3-L1, and its downregulation inhibits adipogenesis. (A) RT-PCR shows no TIP expression in noninduced 3T3-L1 cells and restricted TIP-6 detection after completion of adipogenic induction. (B) Real-time PCR showing time-course expression of TIP-6 and TIP-3. The TIP-6 message increases gradually by day 1, peaking on day 5, whereas TIP-3 is not expressed at any time point. (C) Western blot analysis shows TIP-6 peptide detection by day 1, peaking at day 5. The controls are NIH 3T3 cells transfected with TIP-3 and TIP-6. (D) Time-course expression of C/EBPβ, PPARγ2, and C/EBPα during 3T3-L1 adipogenic differentiation. (E) Suppression of TIP-6 by RNAi significantly inhibited PPARγ2 and C/EBPα expression, with no effect on C/EBPβ. (F and G) TIP-6 inhibition by RNAi inhibited 3T3-L1 adipogenic differentiation. (F) Scale bar = 50 μm. The error bars on top of each column (B, D, E, and G) represent the standard errors.

into NIH 3T3 cells and performed ChIP assays. TIP-6, p300, acetylated H3K9,14, acetylated H4, acetylated H4K16, and RNA polymerase II were detected at the PPARγ2 promoter site by RT-PCR and real-time PCR (Fig. 9A and B). In the absence of TIP-6, p300 was not recruited to the promoter (Fig. 9A and B). In the absence of the SANT domain, TIP-6ΔSANT and p300 were detected at the promoter site, albeit in reduced amounts, but there was no detection of acetylated H3 and H4 or RNA polymerase II (Fig. 9A and B). To determine whether the reduced amount of p300 recruited to the PPARγ2 promoter in the presence of TIP-6ΔSANT could account for the absence of H3/H4 acetylation, we increased the volume of TIP-6ΔSANT transfected into the cells by fivefold in order to increase the amount of p300 in the IP material. Immunoblots confirmed the increment in TIP-6ΔSANT in the IP material (Fig. 9C and D). This resulted in an increase in TIP-6ΔSANT

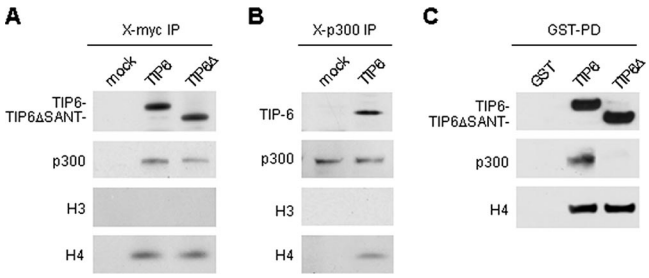


FIG. 8. TIP-6 binds directly and indirectly to p300 and H4. (A) myc-tagged TIP-6 (TIP6), TIP-6ΔSANT (TIP6Δ), and empty vector (mock) were expressed in NIH 3T3 cells, and IPs were carried out with x-myc Ab and immunoblotted for TIP, p300, H3, and H4. TIP-6 coimmunoprecipitates p300 and H4 but not H3. TIP-6ΔSANT also coimmunoprecipitates p300 and H4, but p300 levels are lower (≈50% lower by densitometry) than those in TIP-6 IPs. (B) myc-tagged TIP-6 (TIP6) and empty vector (mock) were expressed in NIH 3T3 cells, and IPs were carried out with x-p300 Ab and immunoblotted for TIP, p300, H3, and H4. p300 coimmunoprecipitates TIP-6 and H4 but not H3. In the absence of TIP-6 (mock), p300 does not coimmunoprecipitate H4. (C) GST pull-downs were done using GST alone, GST–TIP-6 (TIP6) and GST–TIP-6ΔSANT (TIP6Δ) fusion proteins, purified H4, and recombinant p300. TIP-6 binds to p300 and H4. SANT deletion eliminates TIP-6ΔSANT binding to p300 without affecting binding to H4. These experiments were repeated three times with similar results.

and p300 bound to the PPARγ2 promoter, reaching a level similar to that of TIP-6/p300 (Fig. 9C and D). The increment in p300, however, did not result in H3/H4 acetylation. TIP-6 was not recruited to the C/EBPα promoter (downstream of PPARγ) (Fig. 9E and F).

ChIP assays performed on 3T3-L1 cells after adipogenic differentiation demonstrated the recruitment of endogenous TIP-6, along with p300, to the PPARγ2 promoter leading to the acetylation of promoter-associated H3/H4 (Fig. 10A and B). No p300 or acetylated H3/H4 were detected at the PPARγ2 promoter site in the 3T3-L1 cells before adipogenic differentiation (day 0) (Fig. 10A and B). Real-time PCR showed that TIP-6 is not recruited to the C/EBPα promoter (Fig. 10B).

## DISCUSSION

Here we report the TIP family of transcription regulators to be presently composed of eight isoforms featuring the SANT, SAM, and NRB domains characteristic of histone-modifying enzymatic complexes. Our studies indicated that these transcription regulators do not have intrinsic catalytic activity but participate in H3/H4 acetylation through the recruitment of the p300 HAT enzyme. p300 belongs to the MYST family of HATs and acetylates H2A, H2B, H3, and H4 (reviewed in references 13 and 49). p300 interacts either directly or through cofactors with a wide variety of transcription factors, including nuclear receptors (13, 49), and therefore, p300 is considered a nuclear receptor coregulator. p300 also interacts with components of the basal transcriptional machinery (9, 33, 63) and with other proteins (28). p300 has been shown to play essential roles in myogenesis (12, 35, 38, 44, 47, 60) and adipogenesis (18, 53), the two processes respectively induced by TIP-1 and TIP-3. Furthermore, mutations in p300 have been associated with certain cancers and other human disease processes (28).

Among the three functional motifs present in TIPs, the only one common to all isoforms is the SANT domain. Several studies demonstrated that the SANT domain is required for histone-modifying enzymatic complexes to be catalytically active (6, 10, 22, 50). In agreement with these previous studies, the deletion of the SANT domain significantly inhibited TIP-recruited HAT activity.

To further elucidate the functional role of the SANT domain, we focused on TIP-6, the shortest TIP and the only isoform with a $SANT^+$ $SAM^-$ $NRB^-$ makeup. Since TIP-1 ($SANT^+$ $SAM^-$ $NRBa^+$) and TIP-3 ($SANT^+$ $SAM^+$ $NRBb^+$) induced embryonic mesenchymal cells to follow, respectively, a myogenic or adipogenic pathway (26), we determined whether TIP-6, with only a SANT domain, was able to direct NIH 3T3 cell differentiation into a specific mesenchymal cell lineage. We found that the ectopic expression of TIP-6 in NIH 3T3 cells induced adipogenic gene expression without inducing the expression of myogenic genes.

Additional studies further supported a role for TIP-6 in adipogenesis. We found that the transfection of TIP-6 into preadipocytes triggered their maturation into adipose cells. Furthermore, TIP-6 was rapidly induced upon the treatment of 3T3-L1 cells with the adipogenic cocktail, and its downregulation inhibited 3T3-L1 adipogenic differentiation. Of notice, TIP-3, which is expressed in adipose tissue in vivo and induced preadipocyte differentiation in culture, was not detected in the 3T3-L1 cell line. Finally, TIP-6 was present in adipose tissue in vivo.

Adipogenesis has been divided in two phases. The first phase, known as determination, involves the commitment of a pluripotential stem cell to the adipocyte lineage. In the second phase, which is known as terminal differentiation, the preadipocytes take the characteristics of mature adipocytes (43). Some of the transcription factors participating in the adipogenic cascade have been well established. The C/EBPβ and C/EBPδ transcription factors are among the earliest seen. These two proteins induce the expression of the transcription factor/nuclear receptor PPARγ2. The forced expression of PPARγ2 is sufficient to induce adipocyte differentiation in fibroblasts (55) and is therefore considered the "master regulator" of adipogenesis (43). PPARγ2 in turn activates C/EBPα, which feeds back on PPARγ2 to maintain the differentiated state. The transcription factor ADD1/SREBP1 (30) and few other recently identified proteins, including TIP-3 (43), have the ability to directly activate PPARγ2 by inducing its expression and/or by promoting the production of an endogenous PPARγ2 ligand. The activation of this transcription factor cascade leads to the expression of genes that characterize the terminally differentiated fat cell phenotype (43). Within this well-established adipogenic cascade, TIP-6 acts by inducing PPARγ2. Like TIP-3, the other adipogenic isoform, TIP-6 expression is inhibited by stretching. These studies therefore identified TIP-6 as a novel adipogenic factor and added to the notion that TIPs play a significant role in mesenchymal lineage determination.

Interestingly, TIP-6 and TIP-1 amino acid composition is almost identical, and yet one induces adipogenesis and the other myogenesis. The NRBa seems to be a key element for the myogenic effect of TIP-1 since our previous studies showed that, in the absence of the NRBa, a TIP-1 mutant was not

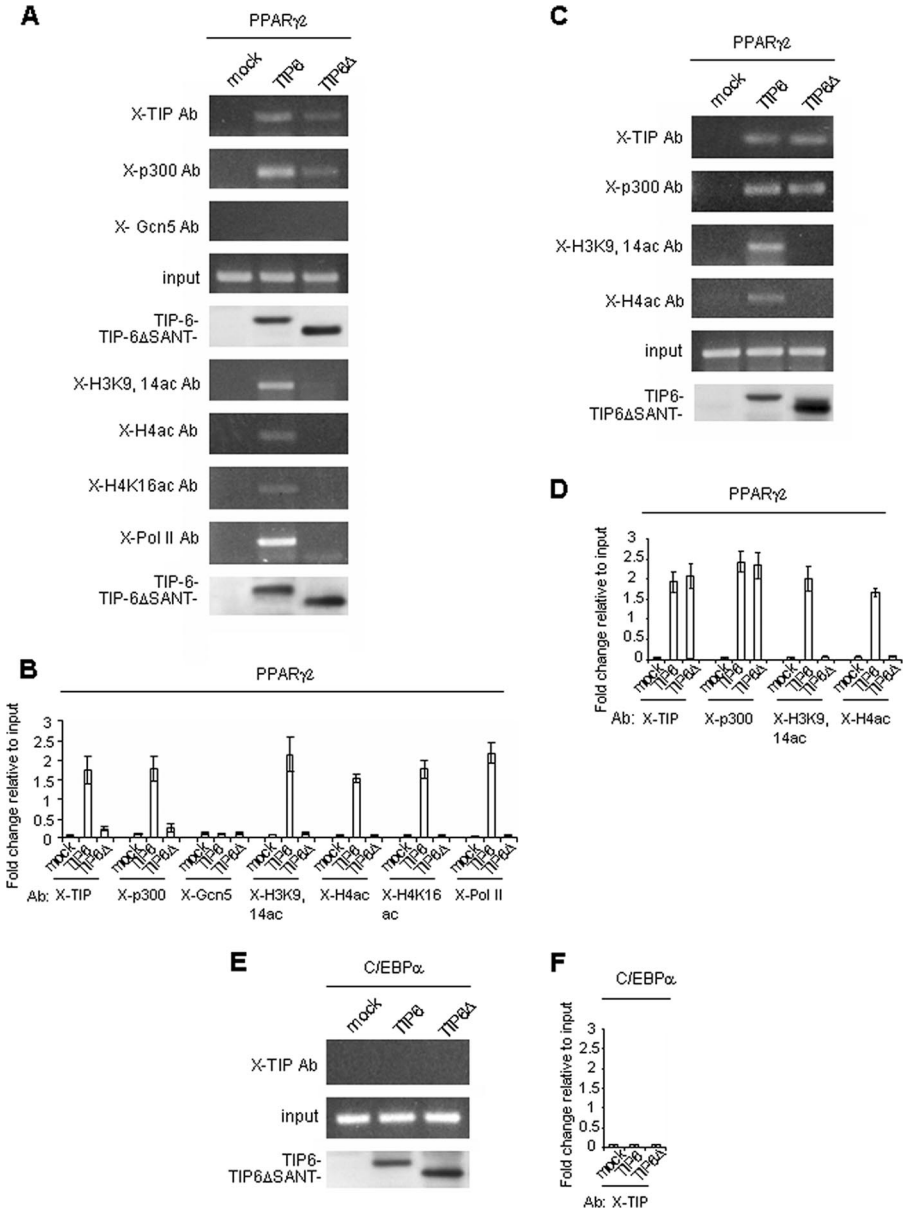


FIG. 9. SANT-mediated direct TIP-6 binding to p300 is required for H3/H4 acetylation at the PPARγ2 promoter. (A and B) myc-tagged TIP-6 (TIP6), TIP-6ΔSANT (TIP6Δ), and empty vector (mock) were expressed in NIH 3T3 cells, and ChIP assays were conducted 48 h after transfection. TIP-6, p300 (but not Gcn5 HAT control), acetylated (ac) H3K9,14, H4 (multiple sites), H4K16, and RNA polymerase II are detected at the PPARγ2 promoter site by RT-PCR (A) and real-time PCR (B). Upon SANT deletion, TIP-6ΔSANT and p300 are still recruited to the promoter site but in a reduced amount; however, acetylated H3/H4 and RNA polymerase II are not detected. The x-myc immunoblot shows the presence of TIP-6 and TIP-6ΔSANT in IP material. (C and D) myc-tagged TIP-6 (TIP6), fivefold more TIP-6ΔSANT (TIP6Δ), and empty vector (mock) were expressed in NIH 3T3 cells, and ChIP assays were conducted 48 h after transfection. ChIP assays show increments in TIP-6ΔSANT and p300 associated with the PPARγ2 promoter resulting from an increase in transfected TIP-6ΔSANT, as show by RT-PCR (C) and real-time PCR (D). The increment in p300 does not result in the acetylation of H3 or H4 in the presence of TIP-6ΔSANT. x-myc immunoblot shows the presence of TIP and TIP-6ΔSANT in IP material. (E and F) myc-tagged TIP-6 (TIP6), TIP-6ΔSANT (TIP6Δ), and empty vector (mock) were expressed in NIH 3T3 cells, and ChIP assays were conducted 48 h after transfection. RT-PCR and real-time PCR show that TIP-6 is not recruited to the C/EBPα promoter (downstream of PPARγ2). The x-myc immunoblot shows the presence of TIP-6 and TIP-6ΔSANT in IP material. The error bars on top of each column (B, D, and F) represent the standard errors.

recruited to the SRF promoter but was associated instead with the PPARγ2 promoter and induced adipogenesis (26).

In those histone-modifying enzymatic complexes bearing SANT domains in noncatalytic subunits, such as is the case for TIPs, their SANT domains have been shown to directly interact with the catalytic subunit (22, 50, 61, 65), with histones (10, 62), or with both (50). We found that TIP-6 directly interacts with both and that TIP-6 binds to p300 in a SANT-dependent manner and to H4 in a SANT-independent mode. TIP-6 does not interact directly with H3. Since the deletion of the SANT

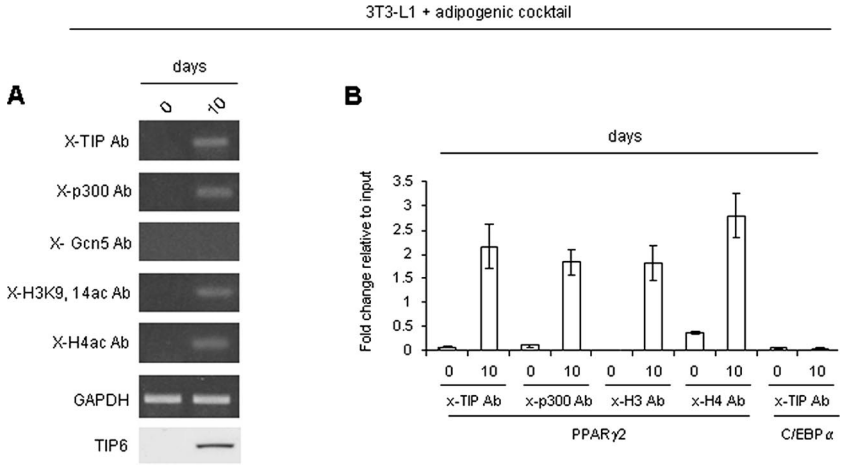


FIG. 10. Endogenous TIP-6, along with p300, are recruited to the PPARγ2 promoter and acetylate H3/H4 at the promoter site. 3T3-L1 adipogenic cells were induced to differentiate, and ChIP assays were conducted at 0 and 10 days after induction. TIP-6, p300 (but not Gcn5 HAT control), acetylated H3K9,14, and H4 (multiple sites) are detected at the PPARγ2 promoter site by RT-PCR (A) and real-time PCR (B). The x-TIP immunoblot shows the presence of TIP-6 in the IP material. Notice that TIP-6 does not bind to the C/EBPα promoter (B). The error bars on top of each column represent the standard errors.

domain diminished but did not completely abrogate TIP-6ΔSANT-p300 association, our data suggested that TIP-6 and p300 are subunits of a larger enzymatic complex. Preliminary studies indicate that such a complex has a molecular mass of 1.2 MDa, as determined by sizing column. Although the various subunits of most HAT complexes have been well characterized (49), there is no information about p300-associated proteins. The family of TIPs therefore represents the first subunit identified in a p300-bearing HAT complex.

We found that TIP-6 and p300 are recruited to the PPARγ2 promoter leading to H3/H4 acetylation at the promoter site. H3-acetylated sites included H3K4 and H3K19, which are hallmarks of gene activation (23). H4 was acetylated at multiple sites, including at H4K16. H4K16 acetylation has been shown to unravel chromatin in in vitro assays, making it more accessible to proteins involved in transcription activation (48). RNA polymerase II, required for transcription initiation, was also recruited to the PPARγ2 promoter. In the absence of TIP-6, p300 does not occupy the PPARγ2 promoter or associate with H4.

Histone-modifying complexes do not have direct DNA binding activity and therefore require the participation of transcription factors/nuclear receptors to bind to promoters. Although these studies indicated that the bp −361 to +52 portion of the PPARγ2 promoter is the site interacting with the TIP-6–p300 complex, the identity of the transcription factor mediating TIP-6–p300 complex binding to the PPARγ2 promoter is currently unknown. p300 binds to a large number of transcription factors and nuclear receptors (13, 49), but whether any of these binds to the PPARγ2 promoter remains to be elucidated. In addition, TIP-6 may also bind to the mediating transcription factor, as such is the case for c-Myb R2, in which its SANT domain binds to C/EBPs (52) as well as to H3 (40). On the other hand, none of the adipogenic transcription factors demonstrated to bind to the PPARγ2 promoter, namely C/EBPα, C/EBPβ, C/EBPγ, KLF5, KLF15, and SREBP1c (43), had been reported to interact with p300. Nevertheless, the C/EBPs are unlikely to mediate TIP-6–p300–PPARγ2 promoter interaction since neither C/EBPβ nor C/EBPδ is detected in NIH 3T3 cells, before or after TIP-6 transfection, and C/EBPα is secondarily induced by PPARγ2. Furthermore, the deletion of the C/EBP binding sites from the PPARγ2 promoter did not abolish its activation by TIP-6 in promoter-reporter assays. Similarly, the deletion of the KLF binding site, the other transcription factor binding site identified on the PPARγ2 promoter (41), also failed to decrease TIP-6-mediated PPARγ2 activation. We did not detect any of the other known adipogenic transcription factors at the PPARγ2 promoter site in TIP-6-transfected NIH 3T3 cells (Badri and Schuger, unpublished).

In the absence of the SANT domain, TIP-6ΔSANT and p300 were recruited to the PPARγ2 promoter site but did not acetylate H3/H4 even after increasing the number of TIP-6ΔSANT/p300-bearing complexes bound to the PPARγ2 promoter by increasing the expression of TIP-6ΔSANT by severalfold. Therefore, our results suggest that TIP-6 promotes H3/H4 acetylation at the PPARγ2 promoter site by bringing enzymes and substrata together through its dual binding to p300 and H4. In the absence of the SANT domain, direct binding between TIP-6 and p300 is lost, and as a consequence, TIP-6 can no longer position p300 in close proximity to H3/H4 to enable their acetylation. The lack of C/EBPβ and C/EBPδ induction by TIP-6 transfection and lack of recruitment to the C/EBPα promoter further indicates that TIP-6 primarily activates PPARγ2 gene expression and that downstream genes are secondarily induced by PPARγ2.

In embryonic mesenchymal cells, the deletion of either the SANT domain or the NRB resulted in the lack of TIP-1/TIP-3 detection at the SRF and PPARγ2 promoter sites (26). This was most likely due to the low p300 levels in embryonic mesenchymal cells relative to those in NIH 3T3 cells (Badri and Schuger, unpublished) and their reduced amenability to transfection. Under these circumstances, the deletion of the SANT domain or the deletion of the NRB resulted in either insuffi-

cient p300-bearing complexes or complexes with a diminished capability to bind and/or remain bound to the promoters.

Since TIP-6ΔSANT-bearing complexes have reduced but not absent p300 subunits, the almost complete inhibition in HAT activity observed in TIPΔSANT HAT assays, in which p300-H3/H4 contact is forced by the nature of the assay, suggests that TIPs may also contribute to optimal p300 catalytic activity. Indirect support for this possibility is that p300 can exist in different conformations (42) and that change in its structure is a potential limiting factor in p300-mediated catalysis in vitro (54).

In conclusion, our studies suggest that TIPs are a family of transcription regulators required for the recruitment of p300 to specific promoters, for positioning p300 in close proximity to promoter-associated H3/H4, and possibly for maintaining p300 in its catalytically active conformation. The TIP SANT domain is essential for the accomplishment of the last two functions. Furthermore, we identified TIP-6 as a new member in the adipogenic cascade, bringing to three the number of TIPs involved in mesenchymal-lineage determination.

## ACKNOWLEDGMENTS

This work was supported by National Heart, Lung, and Blood Institute grants HL-48730, HL-77514, and HL-78752.

## REFERENCES

1. **Aasland, R., A. F. Stewart, and T. Gibson.** 1996. The SANT domain: a putative DNA-binding domain in the SWI-SNF and ADA complexes, the transcriptional co-repressor N-CoR and TFIIIB. Trends Biochem. Sci. **21:** 87–88.
2. **Badri, K. R., S. Modem, H. C. Gerard, I. Khan, M. Bagchi, A. P. Hudson, and T. R. Reddy.** 2006. Regulation of Sam68 activity by small heat shock protein 22. J. Cell. Biochem. **99:**1353–1362.
3. **Baek, S. H., and M. G. Rosenfeld.** 2004. Nuclear receptor coregulators: their modification codes and regulatory mechanism by translocation. Biochem. Biophys. Res. Commun. **319:**707–714.
4. **Balasubramanian, R., M. G. Pray-Grant, W. Selleck, P. A. Grant, and S. Tan.** 2002. Role of the Ada2 and Ada3 transcriptional coactivators in histone acetylation. J. Biol. Chem. **277:**7989–7995.
5. **Bannister, A. J., R. Schneider, and T. Kouzarides.** 2002. Histone methylation: dynamic or static? Cell **109:**801–806.
6. **Barbaric, S., H. Reinke, and W. Horz.** 2003. Multiple mechanistically distinct functions of SAGA at the PHO5 promoter. Mol. Cell. Biol. **23:**3468–3476.
7. **Belaguli, N. S., L. A. Schildmeyer, and R. J. Schwartz.** 1997. Organization and myogenic restricted expression of the murine serum response factor gene. A role for autoregulation. J. Biol. Chem. **272:**18222–18231.
8. **Berger, S. L.** 2007. The complex language of chromatin regulation during transcription. Nature **447:**407–412.
9. **Black, J. C., J. E. Choi, S. R. Lombardo, and M. Carey.** 2006. A mechanism for coordinating chromatin modification and preinitiation complex assembly. Mol. Cell **23:**809–818.
10. **Boyer, L. A., M. R. Langer, K. A. Crowley, S. Tan, J. M. Denu, and C. L. Peterson.** 2002. Essential role for the SANT domain in the functioning of multiple chromatin remodeling enzymes. Mol. Cell **10:**935–942.
11. **Boyer, L. A., R. R. Latek, and C. L. Peterson.** 2004. The SANT domain: a unique histone-tail-binding module? Nat. Rev. Mol. Cell Biol. **5:**158–163.
12. **Cao, D., Z. Wang, C. L. Zhang, J. Oh, W. Xing, S. Li, J. A. Richardson, D. Z. Wang, and E. N. Olson.** 2005. Modulation of smooth muscle gene expression by association of histone acetyltransferases and deacetylases with myocardin. Mol. Cell. Biol. **25:**364–376.
13. **Chan, H. M., and N. B. La Thangue.** 2001. p300/CBP proteins: HATs for transcriptional bridges and scaffolds. J. Cell Sci. **114:**2363–2373.
14. **Chen, D., H. Ma, H. Hong, S. S. Koh, S. M. Huang, B. T. Schurter, D. W. Aswad, and M. R. Stallcup.** 1999. Regulation of transcription by a protein methyltransferase. Science **284:**2174–2177.
15. **Chen, Z., J. I. Torrens, A. Anand, B. M. Spiegelman, and J. M. Friedman.** 2005. Krox20 stimulates adipogenesis via C/EBPbeta-dependent and -independent mechanisms. Cell Metab. **1:**93–106.
16. **Codina, A., J. D. Love, Y. Li, M. A. Lazar, D. Neuhaus, and J. W. Schwabe.** 2005. Structural insights into the interaction and activation of histone deacetylase 3 by nuclear receptor corepressors. Proc. Natl. Acad. Sci. USA **102:**6009–6014.
17. **Darimont, B. D., R. L. Wagner, J. W. Apriletti, M. R. Stallcup, P. J. Kushner, J. D. Baxter, R. J. Fletterick, and K. R. Yamamoto.** 1998. Structure and specificity of nuclear receptor-coactivator interactions. Genes Dev. **12:**3343–3356.
18. **Erickson, R. L., N. Hemati, S. E. Ross, and O. A. MacDougald.** 2001. p300 coactivates the adipogenic transcription factor CCAAT/enhancer-binding protein alpha. J. Biol. Chem. **276:**16348–16355.
19. **Ge, K., M. Guermah, C. X. Yuan, M. Ito, A. E. Wallberg, B. M. Spiegelman, and R. G. Roeder.** 2002. Transcription coactivator TRAP220 is required for PPAR gamma 2-stimulated adipogenesis. Nature **417:**563–567.
20. **Glass, C. K., and M. G. Rosenfeld.** 2000. The coregulator exchange in transcriptional functions of nuclear receptors. Genes Dev. **14:**121–141.
21. **Guelman, S., T. Suganuma, L. Florens, S. K. Swanson, C. L. Kiesecker, T. Kusch, S. Anderson, J. R. Yates III, M. P. Washburn, S. M. Abmayr, and J. L. Workman.** 2006. Host cell factor and an uncharacterized SANT domain protein are stable components of ATAC, a novel dAda2A/dGcn5-containing histone acetyltransferase complex in *Drosophila*. Mol. Cell. Biol. **26:**871–882.
22. **Guenther, M. G., O. Barak, and M. A. Lazar.** 2001. The SMRT and N-CoR corepressors are activating cofactors for histone deacetylase 3. Mol. Cell. Biol. **21:**6091–6101.
23. **Guenther, M. G., S. S. Levine, L. A. Boyer, R. Jaenisch, and R. A. Young.** 2007. A chromatin landmark and transcription initiation at most promoters in human cells. Cell **130:**77–88.
24. **Heery, D. M., E. Kalkhoven, S. Hoare, and M. G. Parker.** 1997. A signature motif in transcriptional co-activators mediates binding to nuclear receptors. Nature **387:**733–736.
25. **Humphrey, G. W., Y. Wang, V. R. Russanova, T. Hirai, J. Qin, Y. Nakatani, and B. H. Howard.** 2001. Stable histone deacetylase complexes distinguished by the presence of SANT domain proteins CoREST/kiaa0071 and Mta-L1. J. Biol. Chem. **276:**6817–6824.
26. **Jakkaraju, S., X. Zhe, D. Pan, R. Choudhury, and L. Schuger.** 2005. TIPs are tension-responsive proteins involved in myogenic versus adipogenic differentiation. Dev. Cell **9:**39–49.
27. **Jimenez, M. A., P. Akerblad, M. Sigvardsson, and E. D. Rosen.** 2007. Critical role for Ebf1 and Ebf2 in the adipogenic transcriptional cascade. Mol. Cell. Biol. **27:**743–757.
28. **Kalkhoven, E.** 2004. CBP and p300: HATs for different occasions. Biochem. Pharmacol. **68:**1145–1155.
29. **Kim, H. J., J. H. Kim, and J. W. Lee.** 1998. Steroid receptor coactivator-1 interacts with serum response factor and coactivates serum response element-mediated transactivations. J. Biol. Chem. **273:**28564–28567.
30. **Kim, J. B., and B. M. Spiegelman.** 1996. ADD1/SREBP1 promotes adipocyte differentiation and gene expression linked to fatty acid metabolism. Genes Dev. **10:**1096–1107.
31. **Kouzarides, T.** 2007. Chromatin modifications and their function. Cell **128:** 693–705.
32. **Kumar, R., R. A. Wang, A. Mazumdar, A. H. Talukder, M. Mandal, Z. Yang, R. Bagheri-Yarmand, A. Sahin, G. Hortobagyi, L. Adam, C. J. Barnes, and R. K. Vadlamudi.** 2002. A naturally occurring MTA1 variant sequesters oestrogen receptor-alpha in the cytoplasm. Nature **418:**654–657.
33. **Kwok, R. P., J. R. Lundblad, J. C. Chrivia, J. P. Richards, H. P. Bachinger, R. G. Brennan, S. G. Roberts, M. R. Green, and R. H. Goodman.** 1994. Nuclear protein CBP is a coactivator for the transcription factor CREB. Nature **370:**223–226.
34. **Li, B., M. Carey, and J. L. Workman.** 2007. The role of chromatin during transcription. Cell **128:**707–719.
35. **Ma, K., J. K. Chan, G. Zhu, and Z. Wu.** 2005. Myocyte enhancer factor 2 acetylation by p300 enhances its DNA binding activity, transcriptional activity, and myogenic differentiation. Mol. Cell. Biol. **25:**3575–3582.
36. **Maksvytis, H. J., C. Vaccaro, and J. S. Brody.** 1981. Isolation and characterization of the lipid-containing interstitial cell from the developing rat lung. Lab Investig. **45:**248–259.
37. **McKenna, N. J., and B. W. O'Malley.** 2002. Combinatorial control of gene expression by nuclear receptors and coregulators. Cell **108:**465–474.
38. **McKinsey, T. A., and E. N. Olson.** 2004. Cardiac histone acetylation—therapeutic opportunities abound. Trends Genet. **20:**206–213.
39. **Min, J., Q. Feng, Z. Li, Y. Zhang, and R. M. Xu.** 2003. Structure of the catalytic domain of human DOT1L, a non-SET domain nucleosomal histone methyltransferase. Cell **112:**711–723.
40. **Mo, X., E. Kowenz-Leutz, Y. Laumonnier, H. Xu, and A. Leutz.** 2005. Histone H3 tail positioning and acetylation by the c-Myb but not the v-Myb DNA-binding SANT domain. Genes Dev. **19:**2447–2457.
41. **Oishi, Y., I. Manabe, K. Tobe, K. Tsushima, T. Shindo, K. Fujiu, G. Nishimura, K. Maemura, T. Yamauchi, N. Kubota, R. Suzuki, T. Kitamura, S. Akira, T. Kadowaki, and R. Nagai.** 2005. Kruppel-like transcription factor KLF5 is a key regulator of adipocyte differentiation. Cell Metab. **1:**27–39.
42. **Qin, B. Y., C. Liu, H. Srinath, S. S. Lam, J. J. Correia, R. Derynck, and K. Lin.** 2005. Crystal structure of IRF-3 in complex with CBP. Structure **13:** 1269–1277.
43. **Rosen, E. D., and O. A. MacDougald.** 2006. Adipocyte differentiation from the inside out. Nat. Rev. Mol. Cell Biol. **7:**885–896.
44. **Roth, J. F., N. Shikama, C. Henzen, I. Desbaillets, W. Lutz, S. Marino, J. Wittwer, H. Schorle, M. Gassmann, and R. Eckner.** 2003. Differential role

of p300 and CBP acetyltransferase during myogenesis: p300 acts upstream of MyoD and Myf5. EMBO J. **22:**5186–5196.
45. **Salma, N., H. Xiao, and A. N. Imbalzano.** 2006. Temporal recruitment of CCAAT/enhancer-binding proteins to early and late adipogenic promoters in vivo. J. Mol. Endocrinol. **36:**139–151.
46. **Shiau, A. K., D. Barstad, P. M. Loria, L. Cheng, P. J. Kushner, D. A. Agard, and G. L. Greene.** 1998. The structural basis of estrogen receptor/coactivator recognition and the antagonism of this interaction by tamoxifen. Cell **95:** 927–937.
47. **Shikama, N., W. Lutz, R. Kretzschmar, N. Sauter, J. F. Roth, S. Marino, J. Wittwer, A. Scheidweiler, and R. Eckner.** 2003. Essential function of p300 acetyltransferase activity in heart, lung and small intestine formation. EMBO J. **22:**5175–5185.
48. **Shogren-Knaak, M., H. Ishii, J. M. Sun, M. J. Pazin, J. R. Davie, and C. L. Peterson.** 2006. Histone H4-K16 acetylation controls chromatin structure and protein interactions. Science **311:**844–847.
49. **Sterner, D. E., and S. L. Berger.** 2000. Acetylation of histones and transcription-related factors. Microbiol. Mol. Biol. Rev. **64:**435–459.
50. **Sterner, D. E., X. Wang, M. H. Bloom, G. M. Simon, and S. L. Berger.** 2002. The SANT domain of Ada2 is required for normal acetylation of histones by the yeast SAGA complex. J. Biol. Chem. **277:**8178–8186.
51. **Sugihara, H., N. Yonemitsu, S. Miyabara, and S. Toda.** 1987. Proliferation of unilocular fat cells in the primary culture. J. Lipid Res. **28:**1038–1045.
52. **Tahirov, T. H., K. Sato, E. Ichikawa-Iwata, M. Sasaki, T. Inoue-Bungo, M. Shiina, K. Kimura, S. Takata, A. Fujikawa, H. Morii, T. Kumasaka, M. Yamamoto, S. Ishii, and K. Ogata.** 2002. Mechanism of c-Myb-C/EBP beta cooperation from separated sites on a promoter. Cell **108:**57–70.
53. **Takahashi, N., T. Kawada, T. Yamamoto, T. Goto, A. Taimatsu, N. Aoki, H. Kawasaki, K. Taira, K. K. Yokoyama, Y. Kamei, and T. Fushiki.** 2002. Overexpression and ribozyme-mediated targeting of transcriptional coactivators CREB-binding protein and p300 revealed their indispensable roles in adipocyte differentiation through the regulation of peroxisome proliferator-activated receptor gamma. J. Biol. Chem. **277:**16906–16912.
54. **Thompson, P. R., H. Kurooka, Y. Nakatani, and P. A. Cole.** 2001. Transcriptional coactivator protein p300. Kinetic characterization of its histone acetyltransferase activity. J. Biol. Chem. **276:**33721–33729.
55. **Tontonoz, P., E. Hu, and B. M. Spiegelman.** 1994. Stimulation of adipogenesis in fibroblasts by PPAR gamma 2, a lipid-activated transcription factor. Cell **79:**1147–1156.
56. **Torchia, J., D. W. Rose, J. Inostroza, Y. Kamei, S. Westin, C. K. Glass, and M. G. Rosenfeld.** 1997. The transcriptional co-activator p/CIP binds CBP and mediates nuclear-receptor function. Nature **387:**677–684.
57. **Wang, H., Z. Q. Huang, L. Xia, Q. Feng, H. Erdjument-Bromage, B. D. Strahl, S. D. Briggs, C. D. Allis, J. Wong, P. Tempst, and Y. Zhang.** 2001. Methylation of histone H4 at arginine 3 facilitating transcriptional activation by nuclear hormone receptor. Science **293:**853–857.
58. **Yan, H., E. Aziz, G. Shillabeer, A. Wong, D. Shanghavi, A. Kermouni, M. Abdel-Hafez, and D. C. Lau.** 2002. Nitric oxide promotes differentiation of rat white preadipocytes in culture. J. Lipid Res. **43:**2123–2129.
59. **Yang, Y., S. Beqaj, P. Kemp, I. Ariel, and L. Schuger.** 2000. Stretch-induced alternative splicing of serum response factor promotes bronchial myogenesis and is defective in lung hypoplasia. J. Clin. Investig. **106:**1321–1330.
60. **Yao, T. P., S. P. Oh, M. Fuchs, N. D. Zhou, L. E. Ch'ng, D. Newsome, R. T. Bronson, E. Li, D. M. Livingston, and R. Eckner.** 1998. Gene dosage-dependent embryonic development and proliferation defects in mice lacking the transcriptional integrator p300. Cell **93:**361–372.
61. **You, A., J. K. Tong, C. M. Grozinger, and S. L. Schreiber.** 2001. CoREST is an integral component of the CoREST-human histone deacetylase complex. Proc. Natl. Acad. Sci. USA **98:**1454–1458.
62. **Yu, J., Y. Li, T. Ishizuka, M. G. Guenther, and M. A. Lazar.** 2003. A SANT motif in the SMRT corepressor interprets the histone code and promotes histone deacetylation. EMBO J. **22:**3403–3410.
63. **Yuan, W., G. Condorelli, M. Caruso, A. Felsani, and A. Giordano.** 1996. Human p300 protein is a coactivator for the transcription factor MyoD. J. Biol. Chem. **271:**9009–9013.
64. **Zehentner, B. K., C. Dony, and H. Burtscher.** 1999. The transcription factor Sox9 is involved in BMP-2 signaling. J. Bone Miner. Res. **14:**1734–1741.
65. **Zhang, J., M. Kalkum, B. T. Chait, and R. G. Roeder.** 2002. The N-CoR-HDAC3 nuclear receptor corepressor complex inhibits the JNK pathway through the integral subunit GPS2. Mol. Cell **9:**611–623.
66. **Zhu, Y., C. Qi, J. R. Korenberg, X. N. Chen, D. Noya, M. S. Rao, and J. K. Reddy.** 1995. Structural organization of mouse peroxisome proliferator-activated receptor gamma (mPPAR gamma) gene: alternative promoter use and different splicing yield two mPPAR gamma isoforms. Proc. Natl. Acad. Sci. USA **92:**7921–7925.
67. **Zuo, Y., L. Qiang, and S. R. Farmer.** 2006. Activation of CCAAT/enhancer-binding protein (C/EBP) alpha expression by C/EBP beta during adipogenesis requires a peroxisome proliferator-activated receptor-gamma-associated repression of HDAC1 at the C/ebp alpha gene promoter. J. Biol. Chem. **281:**7960–7967.